7   The stability/instability of bubbles and foams

> The paradox is easily explained. Profit-seeking people will take more financial risk when they believe the coast is clear. By taking bigger chances, however, they unwittingly make the world unsafe all over again.
>
> Hyman Minsky, US Economist, Paying the Price for the Fed's Success, The New York Times, www.nytimes.com/200801/27/opinion/27grant.html

7.1   Overview

All foams are thermodynamically unstable due to their high interfacial free energy, the decrease of which causes foam decay. It is well known that there are several different types of mechanisms involved in the stabilization and decay of foams, which has caused a considerable amount of confusion. In the literature there are many conflicting explanations frequently caused by experimental anomalies and the incomplete interpretation of foaming experiments. Another aspect to consider is that the lifetime of a foam can pass through several different stages, and each stage may involve a different type of mechanism. To explain the overall stability in terms of one mechanism is almost impossible, and the interplay of different mechanisms needs to be taken into consideration. During generation, bubbles expand and contract and are subjected to severe vibrations and dynamic disturbances causing distortion of the adsorption layer. During this process, the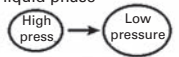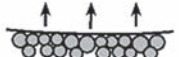 liquid films separating the bubbles are relatively thick and subject to stretching, and viscous elastic forces play a crucial role. Possibly the most important mechanisms for the survival of a wet foam during this stage involves the surface elasticity theories of Gibbs and Marangoni. Gravitational forces also cause fairly rapid drainage to occur during this preliminary stage, but this can be retarded by a high bulk viscosity. On entering a secondary stage, capillary forces come into play causing suction and thinning of the lamellae, and this occurs at a lower rate. In addition, disproportionation may occur causing the diffusion of gas between bubbles. As all these processes occur under dynamic conditions, the equilibrium adsorption coverage is rarely reached.

The process of gas diffusion owes its origins to the difference in pressure, surface tension and curvature of the bubbles, but the gas diffusion to the atmosphere also needs to be considered. In addition to diffusive disproportionation theories to explain the changes in size distribution in bubbles, alternate processes have been considered

which involve the effect of interfacial rheology on the shrinkage of bubbles. As the smaller bubbles are further reduced in size, the adsorption layer becomes compressed during shrinkage, causing an increase in the surface excess (Γ) and a decrease in surface tension. This process would act to counteract shrinking. Under these circumstances, the driving force for disproportionation will also be influenced by the surface dilational modulus of the film. However, bubble shrinkage is usually a fairly slow process, so that the dilational modulus may have sufficient time to relax. At the moment, the role of the surface rheological parameters on diffusive disproportionation remains controversial. At the same time, evaporation, external vibration and shock may occur at the surface of the foam. However, provided the thick films survive drainage, the foam can proceed toward the final state of stability described by the dry foam state. In this final stage, an equilibrium is reached in the formation of the thin lamella films, stabilized by the "disjoining pressure" theories, as discussed in Chapter 3. For well-drained quasi-static foam films (< 100 nm), intermolecular forces become dominant and stability must be discussed in terms of common black films (CBFs) and Newton black films (NBFs). In this chapter the main stabilization mechanisms are reviewed, and these are summarized in Table 7.1. More recently, other stabilizing theories involving partial hydrophobic particles have been under intense study and are discussed in Chapter 8.

Table 7.1 Foam Destabilization/Stabilization Mechanisms

Destabilization mechanisms	Stabilization mechanisms	Stabilization aids
1. Drainage Flow of liquid through foam under gravity	Capillary pressure Fairly thick films Shear viscosity Stratification Thin films Blockage (clogging) Junctions of interconnecting channels Disjoining pressure Thin lamella	High viscosity bulk fluids. Polymeric viscosity enhances (water soluble high m.w polymers; polyacrylamides, EHEC). Coherent mixed surfactant films, proteins. Monodispersed latex or nanoparticles High concentrations of surfactants > CMC Liquid crystals, gels, particle/polymer and particle/surfactant mixtures. Steric and electrostatic repulsion (polymers and charged surfactants). Specific ion effects (Na^+, K^+, Cs^+ and pH control).
2. External vibrations Shock waves	*Gibbs Marangoni* (healing of film) Visco-elasticity surface dilational	High surfactant concentrations > CMC Condensed shells (diglycerols / PE glycols) Hydrophobic, nanopatterning agents (glycose syrups)
3. Disproportionation (*Oswald's* ripening) Gas diffusion through liquid phase	Low solubility gases (low gas diffusion) Air, $N_2 > O_2 > CO_2$	Bubble soluble gas through perfluorohexane type vapours or use surfactant to control type of film. (Common black or Newton black films)
4. Evaporation, temperature gradients, humidity	Temperature and humidity control	Well packed coherent dense packed molecular films

7.2   Classification of the stability of foams

Clearly, there is a sharp distinction between the rates of decay of different types of foams and, for convenience, the instability can be classified into the following different types: (I) unstable or transient foams with lifetimes of seconds or even less; (II) metastable foams with lifetimes of hours or even days; (III) high stability foams which exhibit stability of the order of weeks or a few months; (IV) ultra-stable foams which are stable for at least 6 months and in some cases for years. There is an industrial demand for high-stability foams, particularly in the manufacture of polymers, materials and metal foams.

7.2.1   Unstable (transient) foams

Champagne is a classic example of an unstable foam (Fig. 7.1(a)). Some sea foams also last for only a few seconds, whereas foams produced in turbulent rivers and streams can persist a little longer. Transient foams are also generated in solutions of inorganic electrolytes such as NaCl. Mild surfactants such as short-chain alcohols (ethyl, propyl, isobutyl, etc.) aniline, phenol, pine oil and short-chain undissociated fatty acids (formic, propionic) belong to this group and are considered to be weak foaming agents. These compounds are usually sparingly soluble in water and generate a low degree of surface elasticity and rupture fairly easily. The lifetime of these unstable foams is sensitive to the concentration of the surfactant, and a maximum stability tends to occur at some critical concentration. The foamability of transient foams can be explained by weak surface tension gradients and the Gibbs–Marangoni effect, which will be discussed in a later section of this chapter.

Fig. 7.1   Transient foams (champagne) are dynamic, with lifetimes in seconds, whereas static foams such as beer have lifetimes of hours. Drainage and disproportionation occur in both systems, but the beer foams are stabilized by proteins which induce steric disjoining pressure interactions between the lamellae.

7.2.2 Metastable foams

These foams are capable of withstanding ordinary disturbances, such as thermal or Brownian fluctuations, but they usually collapse in an irregular manner due to abnormal disturbances such as evaporation and temperature gradients. Many surfactant systems produce metastable foams at fairly high concentrations (near or above the CMC). Generally, the lifetimes increase exponentially with concentration of surfactant, and a plot of foam lifetime versus concentration often produces an S-shaped profile. This plot becomes steep beyond a critical concentration, and usually a maximum stability is reached which corresponds to the Plateau region on the curve. In these systems, the thin film drainage times are relatively short (compared to the total foam lifetimes), and the stability is controlled by the balance of interfacial forces, which equilibrate after film drainage has been completed.

7.2.3 High-stability foams

High-stability foams can be prepared from detergents, mixtures of oppositely charged surfactants (anionic and cationic surfactants), surfactant/particle mixtures, etc. In other cases, the systems are stabilized by high molecular weight polymers or water-soluble proteins. In these systems, steric interfacial forces play an important role in preventing thin film rupture. Beer foams are essentially polypeptide foams, and a "Guinness" foam (Fig. 7.1(b)) is a typical example of a thermodynamically (sterically) stabilized system where disproportionation and coalescence occur slowly.

7.2.4 Ultrastable foams

These foams are extremely stable and may be produced from xanthate gums, proteins (hydrophobins), partially hydrophobic particles, mixtures of silica nanoparticles and short-chain surfactants. Usually, these types of surfactant systems produce bulk aggregates, soft or crystalline entities which compact in the Plateau borders and arrest drainage. The foams are fully stable against disproportionation and coalescence. Also, gel formation of solids play an important role in these systems, particularly in surfactant/nanoparticle mixtures that arrest drainage and gas diffusion.

7.3 Reversing the stability of foams

In certain industrial processes, the stability of the foam needs to be tuned for specific performance requirements. For example, there is an initial requirement for a surfactant with strong foaming action, but, at a later stage in the process, the foam needs to be reduced or suppressed without the use of defoaming agents. This is the case in the cleaning of radioactive vessels, where a good foaming agent can be applied to remove particles from the walls of the vessel, but then the foam needs to
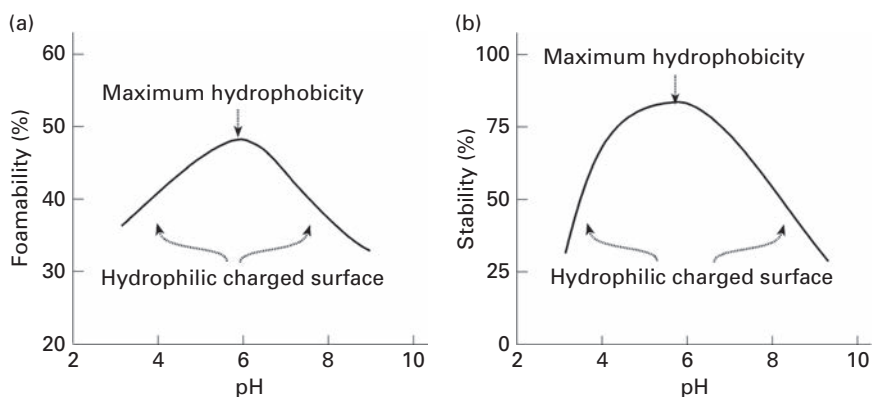
Fig. 7.2   Foamability (determined by the maximum foam volume after 10 s of gas flow at a constant flow rate of 5 ml/s) versus pH and (b) foam stability (after 300 s standing) versus pH. From ref (2).

be destroyed releasing a small volume of contaminated liquid. Reversibility or regeneration can be achieved by applying a simple trigger mechanism, which can involve a change in pH, temperature, UV radiation or changes in the aggregated state of the foaming agent.

7.3.1   pH-responsive foams

A pH-responsive foam often involves a change in stability with change in pH region. In 2007, Binks and coworkers (1) developed a pH-responsive foam system using colloidal polystyrene latex particles stabilized by polyacrylic acid. These particles had an isoelectric point (pH$_{iep}$) of 3.5. The particles were found to strongly adsorb on the bubbles, enabling stable foams to be easily generated at low pH (< 3.5) where the surfaces are partially hydrophobic with only a slight positive charge. At high pH, where the particles were negatively charged (hydrophilic surfaces), no foaming was observed, but by decreasing the pH and suppressing the charge, foams could be regenerated. Alternatively, protein surfactants can be used, and in 2012, Engelhardt and coworkers (2) carried out experiments with a bovine serum albumin (BSA) protein. The adsorption was related to the pH$_{iep}$ of the protein (which had a value of about pH 6) and the foaming performance is shown in Fig 7.2.

In this study, vibrational sum frequency generation (SFG) was used to provide specific information on the composition and orientation of the protein molecules adsorbed at the bubble interface, and ellipsometry enabled complementary information on the thickness of adsorbed layer to be obtained. Maximum foamability and foam stability were found to occur in the region of the pH$_{iep}$ and it was suggested that the strongly adsorbed film was partially hydrophobic and consisted of a thick amorphous aggregated network that stabilized the bubbles against disproportionation, and retarded the drainage. Above or below the pH$_{iep}$, the particles were less
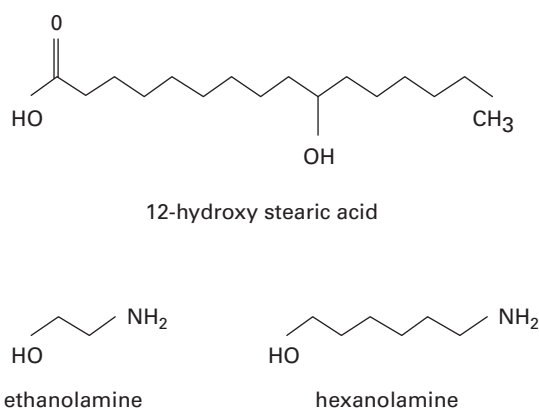
Fig. 7.3   Fatty acid system 12-hydroxyl stearic acid (12-HAS) surfactant which was dispersed in water with an organic counterion (such as ethanolamine or hexanolamine). From ref (4).

hydrophobic, which reduced both foamability and foam stability. In 2011, Middelberg and coworkers (3) found that good foaming occurred in the alkaline pH range for a green biosurfactant protein designated DAMPA4, and a suppression in foaming was achieved through a small pH shift (one unit, from 8.5 to 7.5). The response was found to be reversible.

7.3.2   Temperature-responsive foams

A temperature-responsive aqueous foaming system was developed by Fameau and coworkers (4) in 2011 based on a fatty acid: 12 hydroxyl stearic acid, designated 12-HAS. This was dissolved in water with an organic counterion (etha-nolamine or hexanolamine). The chemical structure of these molecules is shown in Fig. 7.3.

At low temperatures, after handshaking, this surfactant was found to give foams which were stable over weeks and even months. This behavior was explained by the formation of a self-assembly consisting of multi-tubes (10 μm length and 600 nm diameter) which strongly adsorbed at the bubble interface, producing strongly visco-elastic films. Confocal microscopy and SANS analysis indicated that the structural network of tubes restricts the drainage within the lamellae. However, it was also shown that these tubes melt into micelles at higher temperatures, which caused the complete destruction of foam in the presence of both ethanolamine and hexanolamine fatty acid salts. Lowering the temperature caused the tubes to be reformed, and this reversed the foam stability. In a further step, the thermo-responsive 12-HAS tube structures were combined with carbon black particles to create photo-responsive foams (5). On exposure to UV illumination, the carbon black particles in the foam absorb light radiation and act as a photothermal heat converter. This causes the
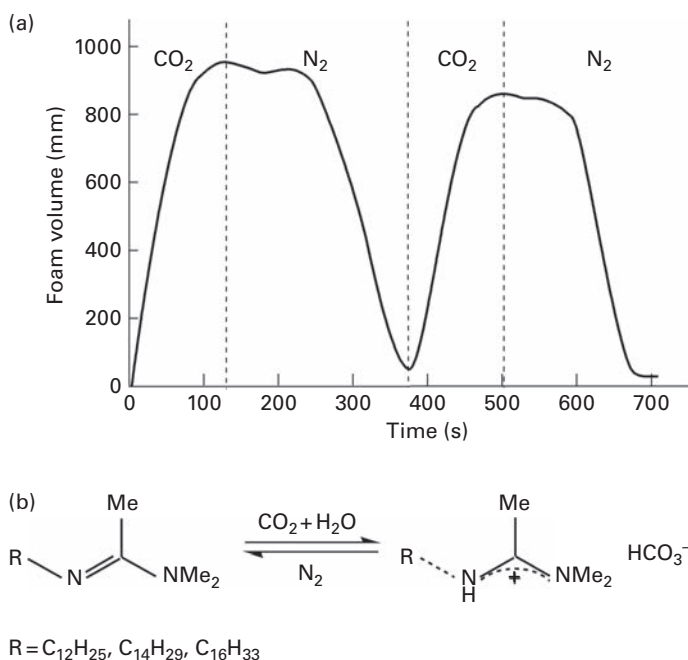
(a)

(b)

$R = C_{12}H_{25}, C_{14}H_{29}, C_{16}H_{33}$

Fig. 7.4   (a) Foam control by diffusing different types of gases through foaming solution. (a) The transformation from stable to unstable foam by changing the type of gas. Two cycles of treatment with CO_2 followed by N_2 are shown. (b) The change in surfactant structure. Bubbling with CO_2 results in the conversion of imidazoline (HEAIs) type surfactant (non-foaming) to the 2-alkyl-1-hydroxylethylimidazolinium carbonate cationic (HEAIBs) type surfactant. From ref (6).

temperature inside the foam to increase, resulting in the transition of tubes into micelles and leading to rapid destabilization. The approach was extended to magnetic particles, producing the first foam to exhibit a thermo-photo-magneto-tunable response.

7.3.3   Gas-responsive foams

It was also found possible to trigger foams generated from a 2-alkyl-1-hydroxy-lethylimidazolinium carbonate cationic surfactant (HEAIB) by alternatively bubbling CO_2 and N_2 through the solution (6). The experiments were carried out in sealed vessels. Interestingly, the foaming behavior was shown to be cyclic (Fig. 7.4 (a)). Initially, on bubbling CO_2 through the solution, the foam volume is shown to sharply increase, reaching a maximum after about 2 minutes and then, after a further 2 minutes, N_2 was bubbled through the solution to remove the CO_2, which suppressed the foaming. It was suggested that the mechanism involved the conversion of the imidazoline HEAI, which is a low foaming surfactant to imidazolium bicarbonates cationic HEAIBs (which is a good foamer). The mechanism is illustrated in Fig. 7.4(b).

The results indicate a lower volume fraction in the second cycles, possibly because this conversion process was not 100% efficient. This type of triggering mechanism was thought to be useful for generating and breaking foams in gas wells, but these foam systems had a disadvantage in that they became unstable at higher temperatures.

7.4 Gibbs–Marangoni effect

Surface tension gradients are essential for a freshly produced foam to survive. However, the main deficiency in the early studies on Gibbs elasticity (as discussed in Chapter 1) was that it applies to thin films, and the rate of diffusion of surfactant from bulk solution to the bubble was neglected. In fact, the Gibbs theory only applies to a hypothetical equilibrium state (i.e. it is assumed that there is insufficient surfactant in the film to diffuse to the surface and lower the surface tension). For thick lamellae, under dynamic conditions, the Marangoni effect becomes important and operates on both expanding and contracting films. The Marangoni effect tends to oppose any rapid expansion or contraction of the surface and may provide a temporary restoring or stabilizing force to thin films, which are susceptible to rupture. In fact, the Marangoni effect is superimposed on the Gibbs elasticity, so that the effective restoring force is a function of the rate of extension, as well as the thickness. The Gibbs–Marangoni effect can also explain the maximum foaming behavior which occurs at a critical surfactant concentration in transient foams, as explained schematically in Fig. 7.5.

If the solution is too dilute, then the greatest possible differential surface tension will only be relatively small and little foaming will occur (Fig. 7.5(a)). In the case of the solution being too concentrated, the differential tension relaxes too rapidly because of the supply of surfactant which diffuses to the surface. This causes the restoring force to have time to counteract the disturbing forces and produce a thinner film (Fig. 7.5(c)), resulting in poor foaming. It is in the intermediate surfactant concentration range that maximum foaming occurs (Fig. 7.5(b)). As yet, there is no clear-cut technique to measure the magnitude of the Marangoni effect, and the theoretical treatment is incomplete. The damping of waves (without changing the wavelength of the ripples) in dilute pure surfactant is believed to be caused by the Marangoni effect, since the surfactant may not impart any significant surface viscosities.

7.5 Interfacial rheology

Although the reduction in surface tension is the main driving force for the generation of foam, it is the rheological properties that impact the stability. During foam generation, it is the expansion and contraction of the air/solution interface under strongly dynamic conditions that prevail, while during drainage, it is the compression, coalescence and disproportionation which are the most important factors. During these processes, the initial equilibrium state becomes distorted, causing the
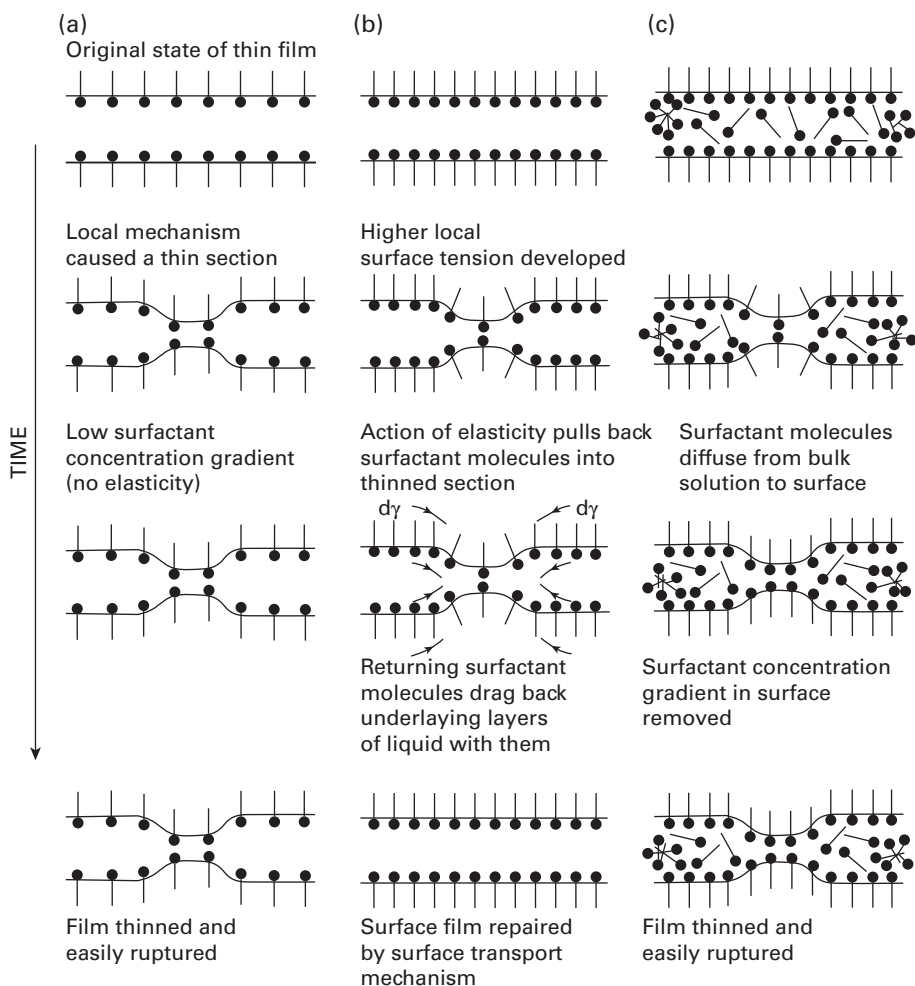
(a)
Original state of thin film

(b)

(c)

Local mechanism
caused a thin section

Higher local
surface tension developed

Low surfactant
concentration gradient
(no elasticity)

Action of elasticity pulls back
surfactant molecules into
thinned section

$d\gamma$ $d\gamma$

Surfactant molecules
diffuse from bulk
solution to surface

TIME

Returning surfactant
molecules drag back
underlaying layers
of liquid with them

Surfactant concentration
gradient in surface
removed

Film thinned and
easily ruptured

Surface film repaired
by surface transport
mechanism

Film thinned and
easily ruptured

Fig. 7.5   Gibbs–Marangoni mechanism of dynamic foam stability. Reaction of a liquid film to a surface disturbance. (a) Low surfactant concentration gives only low differential tension in film and low foaming. (b) Intermediate surfactant concentration. Strong Gibbs–Marangoni effect restores film to original thickness and stabilizes foam. (c) High surfactant concentration (> CMC) differential tension relaxes too rapidly due to diffusion of surfactant. Thinner film formed which can easily rupture.

amphiphiles to dissolve in the bulk solution or adsorb at the interface to restore the equilibrium coverage. Several models were developed for understanding adsorption of surfactant at the surface of bubbles, and two extreme cases were taken into consideration: (a) rapid deformation of the interface so that a non-equilibrium adsorption predominates and (b) slow deformation of the interface such that the adsorption is in equilibrium. In considering the rheology of the interface, different types of deformation occur. The main ones have been classified by (a) the dilational shearing modulus, where the deformation involves an increase or decrease in area of
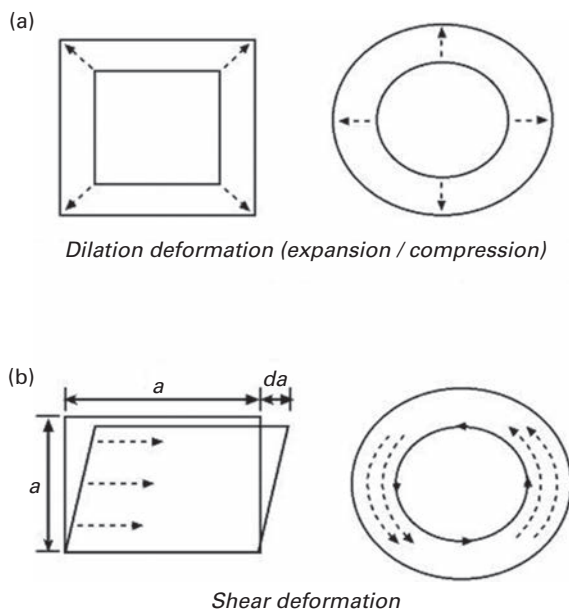
(a)

Dilation deformation (expansion / compression)

(b)

Shear deformation

Fig. 7.6   Examples of a 2D dilational and shear deformation (measured upon expansion/compression) of an interface. From ref (7).

the liquid surface whereas the shape of the area remains the same, and by (b) the shearing deformation, where the shape of the liquid interface is changed while the interface area is kept constant. These processes are illustrated in Fig. 7.6.

External perturbations can cause internal relaxation of the adsorbed surfactant film, and this behavior can give useful information on the dynamics of adsorption layers and the stability of the foam. The drop shape and the capillary pressure tensiometer are suitable methods to measure the dilational rheology of the interfacial layers which define the key properties for understanding the behavior of foams. Dilational elasticity and viscosity are nominated as the important parameters for understanding the dynamic behavior of the interfacial layers. Dilational elasticity of the adsorbed surfactant can be better understood by introducing an intrinsic compressibility of the surface layer. Surface shear rheology provides important information on the structure of the interfacial layer.

7.5.1   Dilational surface viscoelasticity

Although E as presented in Chapter 1 describes the film elasticity in the Gibbs equation, it is a purely thermodynamic quantity, and the experimentally measurable parameters which are needed to characterize the mechanical-dynamical monolayers are the viscoelastic properties (the surface elasticity and surface viscosity). These parameters are coupled and defined by the dilational surface viscoelasticity E^* (also called the interfacial viscoelastic modulus), resulting from the derivation of the

interfacial tension over adsorption ($E^* = d\gamma/d\ln \Gamma$), which also corresponds to the derivation of interfacial tension over bulk concentration ($E^* = d\gamma/d\ln c$). E^* is then dependent on both thermodynamic and kinetic characteristics of the foam systems and may be considered as a dilational or compression modulus (surface stiffness or resistance to deformation) that relates the dilational change in surface area and the resulting change in surface tension. Essentially, surface viscosity reflects the speed of the relaxation processes that restore the equilibrium in the system after imposing stress on it. It is also a measure of the energy dissipation in the surface layer. In contrast, the surface elasticity is a measure of the energy stored in the surface layer as a result of an external stress. However, it is generally difficult to distinguish between the effects on surface viscosity and the surface elasticity, although the steric factors which effect the packing of the mixed film presumably control the rheological behavior of the viscous mixed layers. Isolating the interfacial viscosity is also difficult since the interface is connected to the substrate so that interfacial viscosity is coupled to the bulk viscosity.

In addition to diffusion from the bulk phase, other kinetic processes play a role inside the adsorbed layer, such as orientation, aggregation and compression, and cause rearrangements of the molecular structure. These factors affect E^* and the magnitude of the forces stabilizing the foam films, and, overall, it is difficult to achieve a complete understanding of the surface rheology of soluble and insoluble layers at the interface without knowledge of the shear viscosity, shear elasticity, dilational elasticity, dilational viscosity and transport effects. In 2005, Ivanov (8) carried out a detailed analysis of the range of aspects of interfacial viscoelasticity and concluded that it was impossible to present the exact definition of the surface dilational viscosity. In many cases, the experimentally determined values depended on the interpretation of results and characteristics of the model. At sufficiently high deformation frequencies, E^* may reach a limiting value, which corresponds to a state of equilibrium adsorption where the molecular exchange is suppressed and the adsorption layer will behave as an insoluble monolayer (no diffusion exchange). At much lower frequencies, there is no resistance against area change and the surface remains in equilibrium.

In general, the most interesting region is within intermediate frequency range, which for soluble surfactants is about 1–500 Hz, where relaxation processes take place in and near the interface (e.g. diffusion exchange). This causes viscoelastic surface behavior and, therefore, the viscoelastic modulus E^* has both elastic and viscous components. In the case of sinusoidal deformation in which adsorption and surface tension oscillate around their equilibrium values, the surface dilational modulus is a complex function of frequency. At high surfactant concentrations, the interfacial tension follows the area change with a certain delay due to the various relaxation processes within the interfacial layer and between the interface and bulk solution. In this more general case, the surface behavior is complex and E^* has both elastic and viscous components. In the case of soluble surfactants, the magnitude of the elasticity modulus E is a strong function of frequency of external disturbances. For a more complete understanding of the surface behavior, the complex surface dilational modulus E^* (or visco-elastic modulus) has been expressed in the form of

$$E^* = E' + i \cdot E'' \tag{7.1}$$

where E' is called the storage modulus (dilational elasticity) which is obtained as the pure dilational elasticity and E'' is loss modulus and is proportionate to the viscous contribution where

$$E'' = \omega \eta_d \tag{7.2}$$

and η_d is the surface dilational viscosity and ω the circular or angular frequency. E^* is a complex function, and the molecular interpretation of the dissipative process that gives rise to the imaginary part of the modulus is subject to some controversy. Also, $E^* = d\gamma(t)/dlnA(t)$ where $d\gamma(t)$ and $dlnA(t)$ are incremental changes in surface tension and area, respectively, and η_d is determined by the changes from the phase angle between the generated surface area changes and the response (changes in surface tension). For pure elastic interfaces (insoluble monolayers), the dynamic interfacial tension response $\gamma(t)$ follows the area change $A(t)$ without any phase difference, $\eta_d \rightarrow 0$ and $E^* = E'$.

Bos (9) also stressed the importance of the process kinetics and interfacial rheology in the generation and breakdown of foams. During the generation of foams, new interfaces are produced in a millisecond or less, and time scales with rapid expansion and compression and shear viscosity would probably be more relevant under these conditions. However, high interfacial shear viscosity would probably make a contribution to long-term foam stability. In conditions where bubble break-up occurs, large deformations and high strain rates need to be considered, and since these processes involve large deformations in area (mainly dilational), dilational elasticity and dilational viscosity play important roles. However, the coalescence process is not completely dependent on rheology since activation energies, bending energies and the bulk rheological properties (particularly in high volume fraction and high collision frequencies) play an important role. Under more quiescent conditions, such as when the foam is standing, lower strain rates would be involved. During drainage, several different types of deformation processes may occur. For example, liquid flowing downward due to gravity from the top of the bubble droplet would be subjected initially to dilatation forces, whereas on reaching the bottom will be compressed. In the middle of the droplet, where the distance between bubbles is the narrowest, the interface is subjected to shear deformation. This situation is illustrated in Fig. 7.7. In these circumstances, the overflow cylinder method and the maximum bubble pressure method would possibly be relevant methods of measuring the interfacial elasticity.

7.5.2   Theories and models

Early theories relating to surface elasticity of oscillating systems were developed by Lucassen (7) in 1968 and van den Temple/Hansen (10) in 1965 for a monolayer of surfactant in which the surface elasticity as a function of the surfactant concentration
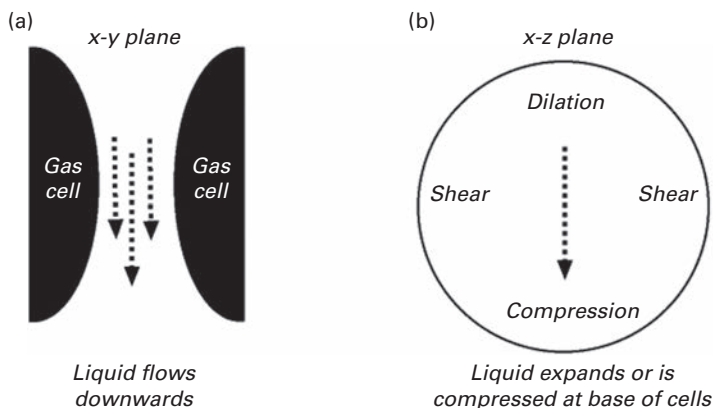
Fig. 7.7   Drainage of a liquid film between two droplets (gas cells); (b) flow types in the droplet (gas cell) interface. From ref (9).

was related to the frequency of the perturbation. This approach led to the establishment of the Lucassen van Temple Hansen (LvdT) model. This was successful in accounting for many surface elastic systems but failed to completely account for the viscoelastic properties of the monolayer. The theory was modified by Wantke and coworkers (11) where a sub-layer was built into the model, and it was assumed that the surface viscoelasticity was associated with a delayed exchange process between the sub-surface and the monolayer. It was also assumed that this exchange process was relatively rapid compared to the deformation rate in surface elastic systems, and this model was found to be useful in describing the data obtained from measurements of surface elasticity and surface viscoelasticity of foam systems. Over recent years, several other models were developed to include underlying dissipative processes such as surfactant re-orientation, surface compression, phase transitions or surface reaction in the surfactant monolayer (12).

7.5.3   Experimental techniques for measurement of elasticity and surface viscosity

Many different methods have been used to investigate the expansion and compression of the air/water interface. These techniques include capillary waves, longitudinal waves, oscillating barriers and oscillating bubbles and can be used at a wide range of different frequencies. They were originally reviewed by Bos (9) but, over recent years, several of these methods have been improved to operate at even higher frequencies. The relevance of the surface dynamic and surface viscosity characteristics were considered with respect to the time of restoring the liquid interface. It was concluded that the former played the more important role close to equilibrium conditions, while the latter was relevant under conditions which were far from equilibrium. These techniques have enabled values of E'' to be determined, and many of these studies have been directed toward studying the influence of the kinetic exchange processes on the dilational

elasticity and the physical interaction between the adsorbed molecules on the surface viscosity.

Surface laser scattering techniques have proved particularly useful for determining the viscoelastic properties of monolayers, and this technique is very sensitive to the behavior at the air/solution interface. When transversal ripples occur, periodic dilation and compression of the adsorbed layer occur which can be studied. This enables the viscoelastic behavior of equilibrium and non-equilibrium monolayers at an air/water interface to be characterized without disturbing the original state of the monolayer. Surface elasticity values were obtained from surface dilational modulus measurements determined at different angular frequencies for films of specific thickness. It is important to consider the thickness and adsorption behavior since these parameters are also inter-related with elasticity. More recently, Derkash and coworkers (13) gave an extended review of the more recent methods of measuring the rheological properties of interfacial layers. Magnetic needle viscometers and rods have also been developed which enable sensitive measurements of the interfacial stress to be achieved (14, 15).

7.5.4   Oscillating bubble methods

Oscillating bubble methods based on the measurement of the variation in surface tension as a response to harmonic compression/expansion of the surface area of a bubble (via variations of the volume) have been well developed and are widely used to measure the surface dilational elasticity. The accuracy of the methods has considerably improved in recent years due to the advancement in high-speed videos and data processing. The oscillating bubble technique was first developed to measure surface dilational elasticity by Kretzschmar and Lunkenheimer (16) working at the Max Planck Institute for Colloids and Interfaces, Potsdam, Germany. This test was originally carried out in the low frequency range from about 10^{-3} to 0.2 Hz. In 2001, Wankte and coworkers (17) modified the method to operate in the 1–300 Hz frequency range. In this method, a small bubble is formed at the end of a capillary tip in a cell and the bubble is subjected to sinusoidal oscillations which are generated from a piezo-element. This causes compressions and expansions of the bubble surface. Changes in bubble radius and surface area produce sinusoidal changes of the pressure in the measuring chamber, and the pressure change is measured by a pressure transducer. As an alternative, the capillary pressure tensiometer measures the capillary pressure directly at higher frequency of 0.1–100 Hz even up to 500 Hz or higher. Both measuring techniques are highly sensitive to the surfactant present at surface and can be used to quantitatively characterize the surface layers. A commercially available instrument known as the bubble profile analysis tensiometer (PAT) has been widely used, and the basic set up together with the profile of the pulsing bubble is shown in Fig. 7.8.

Based on analysis of the oscillations of the bubble shape, values of the dilational interfacial elasticity and information of the surfactant exchange process can be obtained. In Fig. 7.9, the harmonic oscillations of the interfacial surface tension and the drop area
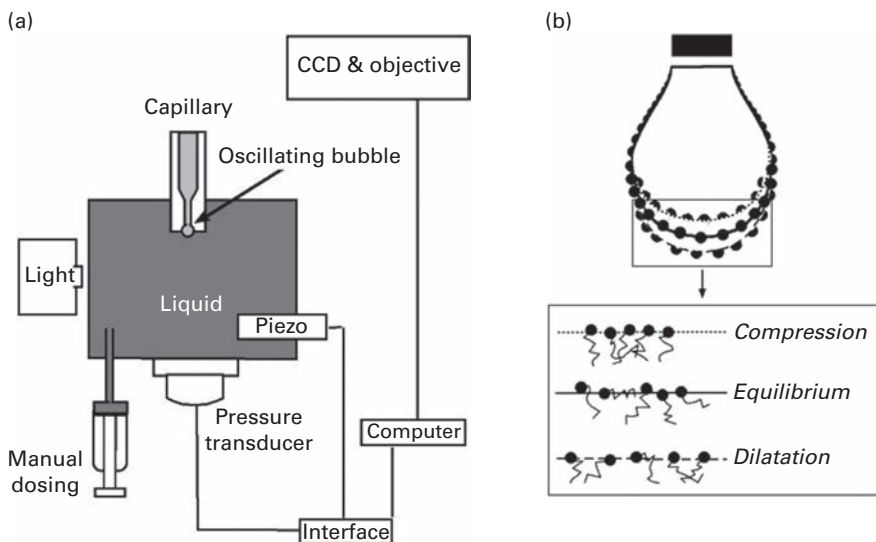
Fig. 7.8   (a) The measuring cell in which the change in surface tension is monitored by capillary pressure measurements and (b) profile of the pulsing bubble showing the adsorption kinetics of the surfactant. Fast oscillation up 100 Hz can be easily achieved.
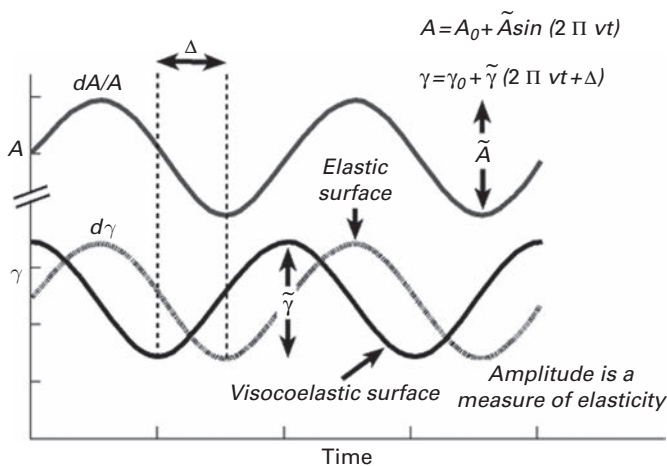

Fig. 7.9   The response to the interfacial tension (γ) and interfacial area (A) to the sinusoidal perturbations of a pendant drop as a function of the component of frequency. For the viscoelastic surfaces the interface storage shear modulus and the interface loss shear modulus can be obtained from the phase difference between the two signals.

obtained at a fixed frequency are shown. In Fig. 7.10, a typical set of results are shown for a surfactant which was measured at three different concentrations.

For a low amplitude harmonic perturbation, the complex dilational viscoelastic modulus or the dilational viscoelasticity E can be expressed by the equation:
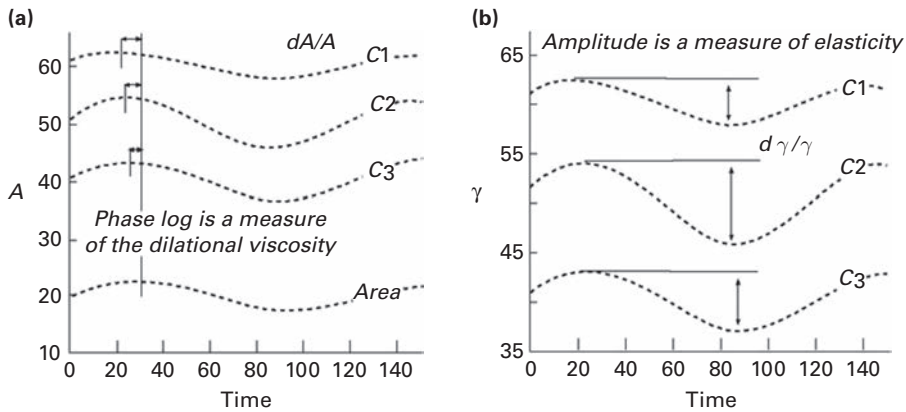
Fig. 7.10   Harmonic oscillations of the interfacial surface tension and the drop area at three different concentrations of surfactant as represented by C_1, C_2 and C_3.

$$E = \frac{\Delta\gamma}{\Delta A/A_0}\pi r^2 \tag{7.3}$$

The complex surface dilational modulus can be obtained from analysis of the amplitude and relative phase shift between the change of area of the bubble image and the change of interfacial tension as a function of time. More in-depth discussions of these techniques are given by Ravera and coworkers (18) in 2010, by Miller and Liggieri (19) in 2005, and Liggieri and coworkers (20). This oscillating bubble instrument has been successfully used at fairly high frequencies, enabling interesting data to be collected on the relaxation mechanisms occurring between the surface layer and adjacent bulk phase within the surface layer. This technique has proved useful in understanding the composition of the interfacial layer and strength of the inter-action between adsorbed species. The pulsating bubble module has also been used to investigate the influence of the surfactant concentration above and below the CMC on E^*. Studies have been reported on a wide range of different types of surfactant systems, including blends of surfactants, polymers and surfactant/poly-mer mixtures (20).

7.5.5   Experimental studies of elasticity and surface viscosity

Although the oscillating bubble method is probably the most widely used technique today, many earlier attempts have been made to try to establish a relationship between the surface rheology and the generation and stability of foams using other methods. This has met with some success, although it appeared to depend on the type of foam and measuring methods. However, it is important to note that the surface rheological measurements are almost always carried out on macroscopic surfaces, and this is often not compatible to the stress and strain in practical foams where turbulence and non-equilibrium conditions can prevail. Early light scattering measurements of the capillary

wave motion of aqueous surfaces covered with fatty acid and lecithin monolayers were reported by Hard and Neuman (21) in 1981. Quantitative determinations of the film dilational elasticity and film dilational viscosity were reported. Viscosity measurements by light scattering were comparable in magnitude to surface viscosities obtained by mechanical (shear) viscometers. Colegate and Bain (22) carried out ellipsometry studies on a liquid jet with a micellar solution of a nonionic surfactant ($C_{14}EO_8$). The results were discussed in terms of the diffusion of micelles to the interface, the adsorption step and the immediate breakdown of the micelles into monomer species. These observations contradicted standard micellar models since it was suggested that the micelles may break down into monomers not only in bulk solution but also in the sublayer before adsorption.

In 2003, Wantke and coworkers (23) measured the surface dilatational properties of aqueous solutions of sodium dodecyl sulfate (SDS) and *n*-dodecanol in the frequency range 1–500 Hz using the oscillating bubble method. It was found that pure dodecanol solution exhibited an elastic surface without viscous effect, whereas the surface of an SDS solution without added dodecanol exhibits a strong viscoelastic behavior. Mixtures showed a graduated transition from elastic to viscoelastic behavior and it was suggested that the dodecanol molecules drive the SDS molecules slowly out of the surface. This study established that a one-component model describing the surface dilatational modulus can be used also for these mixtures. Surface dilational modulus measurements carried out in the mid-frequency range were reported by Anderson and coworkers (24) in 2006. The dynamic state of the surface layer was monitored using a pressure sensor and surface second-harmonic generation (SHG) recorded. The pressure sensor measures the real and imaginary part of the modulus while SHG monitored independently the surface composition (the concentration of soluble surfactant) under dynamic conditions. Two aqueous solutions were studied, a surface elastic and surface viscoelastic solution. The results could be explained by the LvH model, which included a molecular exchange process and provided evidence for a non-equilibrium state within the surface phase.

Recent trends have led to the combination of the oscillating bubble method with other advanced surface analysis techniques. Possible future studies could involve coupling the surface rheology with more precise measurements of the adsorption kinetics, adsorbed amount and surface layer composition. The combination of shear rheometry, ellipsometry and Brewster angle microscope might give more advanced insight into the different mechanisms involved in foaming processes.

7.6   Stability control agents

The stability of foams can be controlled by using single surfactant systems and controlling the aqueous environment by adjustment of pH or by adding inorganic electrolytes to produce specific ion effects. There is also the possibility of adding a second surface-active agent such as a low molecule long straight-chain unbranched
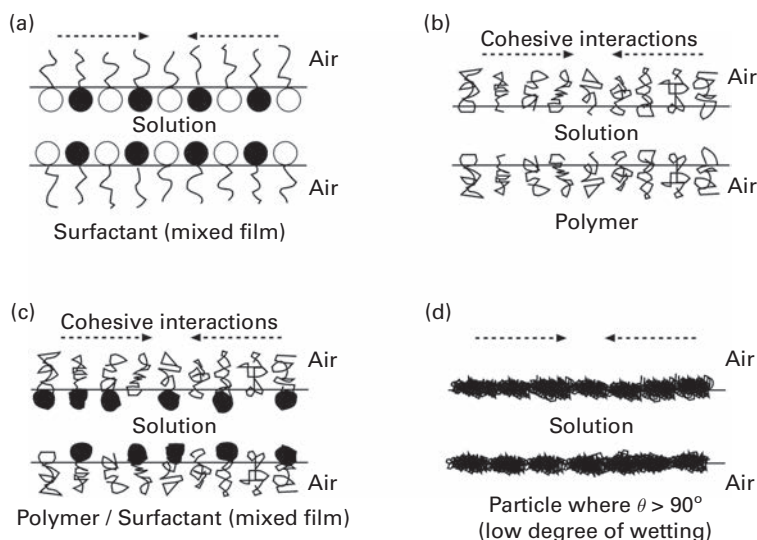
Fig. 7.11 High packing densities result from certain types of mixed surfactant species which can cause strong cohesive interactions similar to polymer or particle films. For example: (a) mixed surfactants system, (b) polymers (c) polymer/surfactant (d) particles with high contact angle attached to the air-solution interface.

hydrocarbon to a polymer or using particles in combination with these chemicals. There are many examples in the literature where mixed surfactant systems such as surfactant/polymers, particles/polymers, etc., have been shown to provide enhanced foam stability, but the complete mechanism for many of these systems has not been completely resolved. Some of these mixed films compared to single component films are shown in Fig. 7.11. However, it has been well known for several decades that these mixtures form coherent surface layers (with high packing densities) which act as an elastic membrane or skin that can stretch and relax. Essentially, the primary effect is thought to be caused by an increase in surface viscosity and elasticity which acts to protect the film against lateral forces produced by disturbances such as thermal fluctuations, evaporation, temperature gradients and external vibrations. Cohesive films are also formed by adding relatively high molar mass polymers, proteins, polysaccharides or certain types of particle. Many food foams are stabilized by protein polymers adsorbed at the air/water interface. However, in recent years it was found that the high mechanical viscoelastic properties associated with coherent films may also reduce thin film drainage.

7.6.1 Single surfactant systems, pH, electrolyte and specific ion effects

As discussed in Chapter 2, the foaming of long straight-chain hydrocarbon ionic surfactant reaches a maximum value around the CMC, but the addition of inorganic electrolytes to the surfactant solution decreases the CMC, enhancing the foaming. Generally, at low electrolyte concentrations, specific adsorption effects change the

magnitude of interfacial charge and electrostatic interactions. This mainly influences the charging of the film, but at high salt concentrations screening of electrostatic repulsion becomes an important mechanism with regard to the stability. It is also important to consider the fact that the type of counterion can affect the degree of dissociation of the surfactant. It has also been well established that the type of counterions and co-ions of the electrolyte has a strong influence on the thickness of foam films and can be used to tune the stability. For example, Schelero and coworkers (25) in 2010 determined the influence of monovalent ions Li^+, Na^+, Cs^+ on the dodecyl salt of SDS. As the size of the cation increased, the adsorption increased, producing thinner and less stable films. In the case of anions, thicker and more stable films are produced which increased the foaming.

7.6.2   Mixtures of surfactants, foam builders/boosters

The formation of coherent films from densely packed layers of adsorbed unbranched surfactant molecules containing long straight-chain hydrocarbons and small terminal polar groups is a basic requirement to obtain stable equilibrium films. For example, it is well known that the mixtures of SDS with dodecylalcohol, and dodecylbenzene sulfonate with lauryl isopropanolamide show improved foaming compared with the single components. Some common impurities present in alkyl sulfates, such as free fatty acid, can act to enhance foam stability, and the mechanism may involve interfacial rheology. Many types of surfactants can be added to enhance the foaminess of weakly foaming systems and they have been designated as foam boosters. This may cause an increase in foamability or an increase in stability or both. In industries foam boosters are often evaluated on an empirical trial-and-error basis, and many different types of surfactants have been screened but only a few have become widely acceptable.

Although nonionic surfactants produce only low or moderate foam volumes when used alone, they act as excellent foam boosters for many anionic systems. It was postulated that stabilizers penetrate the surfactant surface film giving a coherently packed surface film, and straight-chain surfactants give more foam promotion than branched chain surfactants. According to early studies by Schick and Schmolka (26), the order of susceptibility to foam promotion follows the order of decreasing van der Waals forces between the straight-chain hydrophobe of the stabilizer and the hydrophobe of the adjacent surfactant. This order may be expressed as

*primary alkyl sulfates > 2-*n-*alkane sulfonates, secondary alkyl sulfates> alkyl benzene sulfates > branched-chain alkyl sulfonates.*

Foam boosters at fairly high concentrations may also increase the bulk viscosity and possibly the foam liquid network and may be associated with formation of liquid crystals. On the other hand, additives which defer or destroy liquid crystalline structures, such as short or branched alcohols, promote drainage and decrease stability.

Table 7.2 Correlation between foam stability and CMC lowering by additives for sodium 2-*n*-dodecylbenzene sulfonate solutions. From ref (25).

Additive	CMC (g/L)	Foam stability	
		Decrease in CMC (%)	Foam volume (ml) after 20 min.
None	0.59		18
Lauryl glycerol ether	0.29	51	32
Laurylethanolamide	0.31	48	50
n-Decyl glycerol ether	0.33	44	34
Laurylsulfolanylamide	0.35	41	40
n-Decyl-3-sulfolanyl ether	0.35	41	28
n-Octyl glycerol ether	0.36	39	32
n-Decyl alcohol	0.41	31	26
N-(3-Sulfolanyl)oleylamide	0.48	19	23
Caprylamide	0.50	15	17
Lauryl chlorohydrin glycerol ether	0.57	3	22
Tetradecanol-2	0.60	0	12

Further, a correlation between CMC lowering and foam stability indicates that the more effective stabilizers are those which cause the greatest lowering of the CMC. An early systematic study by Schick and Fowkes (27) with a series of different detergents, showed the importance of different additives on reducing the CMC. From this work it can be concluded that the additives which had the greater influence in reducing the CMC were the most effective foam stability boosters. The additives with unbranched paraffin chains (which were equal in length to the detergent molecule) and that had highly hydrophilic nonionic polar groups at one end were the most effective. This can be illustrated by the effect of different types of surfactants on the stability of sodium 2-*n*-dodecylbenzene sulfonate, are shown in Table 7.2.

Other effective foam enhancers or boosters include alkanolamide-type surfactants. Sanders and Knaggs (28) reported that these types of additives were extremely effective in practical systems. Early studies suggested that extremely closely packed layers are formed in the mixed surfactant films containing alkanolamides due to the formation of multiple hydrogen bonds, which improves the rheological properties. Rodriguez and coworkers (29) carried out an extensive phase study and small-angle X-ray scattering with an alkanolamide-type foam booster, dodecanoyl N-methyl ethanolamide (NMEA-12). The structure of the surfactant is shown in Fig. 7.12.

This surfactant was reported to have a lower melting point (compared to other alkanolamides) and formed a lyotropic liquid crystalline phase at room temperature which was attributed to an attached methyl group. This increases the fluidity of the molecule. In SDS/NMEA-12 system, wide hexagonal and lamellar liquid crystalline regions were detected at relatively low surfactant concentrations. For both the SDS and the $C_{12}EO_8$ surfactants, the addition of NMEA-12 caused the effective area per molecule
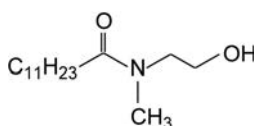
Fig. 7.12   Chemical structure of dodecanoyl N-methyl ethanolamide.

to shrink, producing a tightly compact layer which correlated with the foam booster characteristics.

Foam boosters are needed in detergent, body-care shampoos and hair-conditioner formulations which are mainly stabilized by anionic surfactants. In these systems, oil droplets from grease from the body or hair become dispersed in solution and act as antifoamers. It is often necessary to add an amphoteric and nonionic cosurfactant to suppress the antifoam effects of oil. Basheva and coworkers (30) evaluated a series of surfactants as potential as a foam boosters in the presence of a model detergent system containing silica oil. The surfactants included lauryl amide propyl betaine (LAPB), lauryl acid diethanol amide (LADA), lauryl alcohol (LA) and a glycerine-based nonionic. The weakly foaming solutions contained a commercial anionic surfactant (sodium dodecyl polyoxyethylene-3-sulfate (SPD 3S)), and the silicon oil droplets were dispersed in foaming solution as micrometer-sized droplets. From thin lamellae film experiments, it was shown that the enhanced foam stability in the presence of LAPB and LA correlated with the energetics required to overcome the entry of the oil drop into the air/water interface. It was also shown that the size of the silicone droplet had a significant effect on foam stability and that droplets above about 5 microns caused foam destruction. The mechanism involved the compression of the droplets by walls of the Plateau channels. This resulted in a reduction in film thickness during drainage.

7.6.3   Polymer/surfactant mixtures

The interactions between surfactants and polymers have been extensively covered in a book entitled *Polymers and Surfactants in Aqueous Solution* edited by Holmberg and coworkers (31). Numerous experiments have been reported with different systems, but, due to the wide diversity of the components in these mixtures, it has been difficult to buildup a complete explanation of the relevant mechanisms involved in their application as foam stabilizers. On mixing a surfactant with polymer, frequently the onset of binding or the start of the attachment of the premicellar aggregates on the polymer chain occurs at a critical concentration. This has been designated "the critical aggregate concentration" (CAC) and the value of the CAC is at a significantly lower concentration than the CMC of the pure surfactant. It is also independent of the polymer concentration and, as the polymer concentration decreases, the CAC approaches the CMC of the surfactant. Many studies have been made with mixtures of an ionic surfactant and a nonionic polymer leading to complex formation, and other types of interactions have
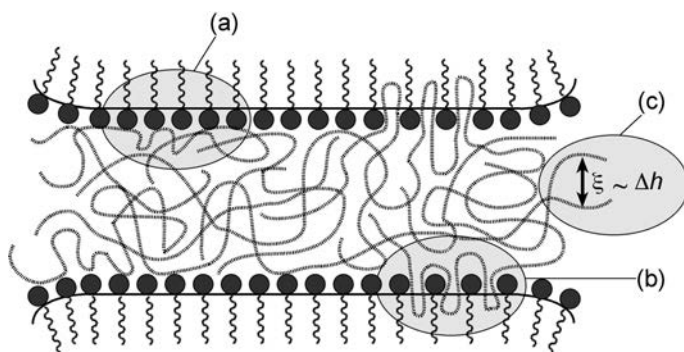
Fig. 7.13 Mixed polyelectrolyte/surfactant film with (a) adsorbed polymer on the surface (b) via formation of surfactant/polymer complexes or (b) via hydrophobic attraction and (c) mesoscopic structured poylectrolytes chains in the film bulk. The distance Δh between the neighboring branches is independent of the kind of surfactant but differs with the kind of polyelectrolyte. From ref (32).

been shown to be involved (31). These have been shown to include (a) the redistribution of the surfactant between the bulk solution and the coil regions, with the surfactant molecules bound individually along the chain, (b) surfactant molecules clustered around hydrophobic sites on the polymer and (c) polymer molecules wrapped around surfactant micelles in such a way that the polymer segments partially penetrate and wrap around the polar headgroup regions of the micelles. It has also been suggested that electrostatic interactions are important in these systems, and the adsorption of these types of complex species at the interface has an important influence on the foaming.

Klitzing and Muller (32) reviewed the different parameters involved in stabilizing binary polymer/surfactant films under dynamic and static conditions. The importance of intermolecular interactions, including DLVO and steric forces, was considered for relatively low and high molecular weight amphiphilic mixtures. The influence of the complex architecture of the polymers in the case of block copolymers and tri-copolymers was discussed in terms of electrostatic screening effects and coiling of the grafted chains. These factors were particularly important under high ionic strength conditions. Fig. 7.13 indicates the different types of interaction which may occur within a thin foam film.

It has also been well established that surface complexes formed below and above the CAC can cause a synergistic lowering of surface tension in these systems. In some cases above the CAC, the stability becomes even higher due to the formation of gel-like structures in the thin film. An overview documenting the different interactions involving combinations of polyelectrolytes and surfactant with different charges was published by Langevin and coworkers (33) in 2001. It is well known that with mixtures of cationic and anionic polyelectrolytes, the thin film stability can be enhanced, particularly if one species is only slightly charged. However, in addition to electrostatic interactions, hydrophobic interactions and hydrogen bonding can also play a role in complex formation. With polymer/surfactant interactions, an increase in polymer concentration above CAC may cause desorption of complexes from the interface which will

destabilize the film and reduce the foaming stability. For many industrial applications, cellulose polymers are used in mixed formulation with low molecular weight surfactants, and it is often necessary to optimize the formulation in order to prevent foaming.

Guerrini and coworkers (34) studied the interactions of an amino-alkyl carbonyl cellulose derivative with SDS and reported that maximum foaming occurred in the region where the charge of the polymer/surfactant complex was neutralized. Precipitation was also reported to occur in this concentration range. For mixtures of a SDS surfactant and an ethyl hydroxyl cellulose (EHEC) polymer, Djuve and coworkers (35) showed that the formation and adsorption of complex polymer/surfactant aggregates at the interface had a pronounced effect on foam stability in aqueous solution. The driving force of the interaction has been discussed in terms of the hydrophobic interactions and the electrostatic interactions between polar SDS and the EHEC polymer. In these systems, a synergism in foaming was established. This behavior was explained by the adsorption of aggregates at the air/water lamellae interface leading to the formation of a coherent gelatinous layer which reduced drainage.

In 2011, Langevin and coworkers (36) reviewed the stability and drainage of free suspended film stabilized by surfactant/polymer mixtures, and in this paper, particular attention was paid to protein systems. Proteins alone are known to form brittle monolayers at the air/water interface that can easily break and leave unprotected areas. However, for mixed surfactant/protein films, the hydrophilic sections and neutral hydrophobic segments can produce compact aggregates which may also partially unfold at interface. In the case of a mixed monolayers produced from surfactants and rigid polyelectrolytes of opposite signs, the surfactants may transform the rigid proteins layer into more flexible and mobile entities that might be capable of responding to applied stress without rupturing. This may be the reason why protein/surfactant film mixtures are more stable than surfactants alone. There is also a possibility that at high surfactant concentration, the proteins may be displaced toward the film interior. From optical observations of the thin films containing proteins, it could be suggested that the inhomogeneous films consisted of gel-like aggregates, and interferometry showed different colors indicating a wide variation of the film thickness. The adsorption of the aggregated proteins also corrugated and deformed the surface, and their confinement in the film possibly provides a gel-like jamming behavior. This prevented measurements of the disjoining pressure between the interfaces of the thin films, but it has been shown by Bergeron and coworkers (37) that it was possible to relate visually the surface characteristics of its the film to the stability. Gel-like structures were observed within critical concentration levels in thin film produced from polyelectrolytes with opposite charge. For example, the thin film images produced from the PAMPS and DTAB systems are shown in Fig. 7.14. These were reported to be extremely stable and near to the precipitation limit of the complex.

Gel-like structures have also been observed in films produced from sodium caseinate (Fig. 7.15). It was reported that the inhomogeneities in such films are mobile at low concentration but become more strongly attached and static at higher
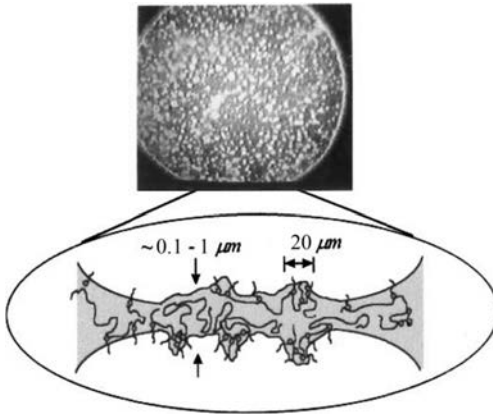
Fig. 7.14   Image of a film made from PAMPS and DTAB at a concentration near the precipitation boundary (top and bottom: Schematic illustration of the film structure). From ref (37).
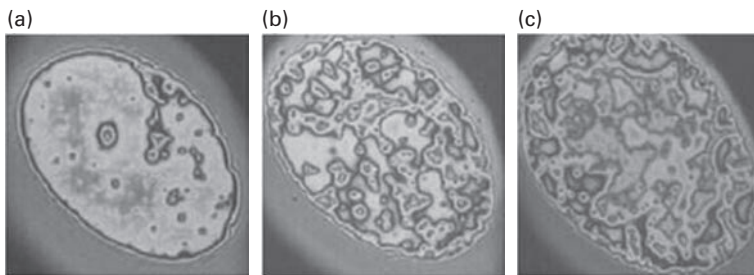

Fig. 7.15   Top view of casein thin films for three different casein bulk concentrations (a) c = 0.05 g/l, (b) c = 0.3 g/l and (c) c = 0.83 g/l and showing heterogeneous thickness and the presence of aggregates. The films become stable as soon as the aggregates percolate. From ref (37, 38).

concentrations (> 0.1 g/l, which corresponds to the stability threshold of foams generated with these solutions).

In industries, frequently mixtures of oppositely charged surface-active agents (anionic and cationic surfactants and surfactant mixtures) are used in foaming formulations; for example, mixtures produced from xanthane-gums, proteins, mixtures of partially hydrophobic silica nanoparticles and short-chain amine surfactants. These mixtures are sometimes referred to as catanionics. Usually these types of mixtures produce bulk aggregates or soft entities which compact in the Plateau borders of the foam preventing drainage.

Many basic research experiments using self-supporting foam films have been used to study these systems. Schelero and von Klitzing (39) prepared foam films with a mixture of a cationic surfactant (alkyl trimethyl ammonium bromide, C_nTAB) and variable amounts of anionic surfactants. Three different types of anionic surfactants with head groups of different size and charge (sodium decanoate, sodium sulfate and sodium styrene sulfate) were investigated. From these studies it was observed that with increasing concentration of the anionic surfactant the film thickness and stability decreased to

a minimum value that was dependent on the type of head group interaction, as well as the hydrophilic/hydrophobic balance of molecules. Stronger interactions, due to hydrophobic interactions and the head groups, appeared to dominate the synergism. From the study it could be suggested that the amount and type of anionic surfactant could be adjusted to tailor the stability of the foam. Also, surface tension was confirmed as a useful technique to study these systems.

7.6.4   Condensed shells

In 2008, Shen and coworkers (40) reported that it was possible to stabilize microbubbles with a mixture of saturated long-chain mono and diglyceride; sodium stearoyl-2-lactylate (SSL-2) in combination with polyethylene glycol (PEG-40 stearate). Langmuir trough studies on monolayers and fluorescence microscopy were combined; this enabled the surface tension, interfacial elasticity modulus, phase behavior and microstructure of the monolayer shells coating microbubbles to be characterized. It was suggested the components were squeezed out to form compact, collapsed aggregates which resulted in the formation of a microbubble shell surrounding the bubbles. The compacted shell was reported to be composed of a condensed phase of low surface tension mono- and diglycerides mixtures with some of the PEG40S and SSL2 remaining trapped between the condensed phase domains.

7.6.5   Nanopatterning

In 2008, extremely stable microbubbles (stable for over 1 year) were prepared by Dressaire and coworkers (41) from a solution of sodium stearate which was dispersed and sheared in a highly viscous glucose syrup phase. The enhanced stability has been explained by the formation of an elastic condensed surfactant phase with hexagonal domains buckled outward from the bubble covered surface. It was suggested that it was the elastic response of the interface which prevented the shrinkage of the bubbles. The systems were found to have a wide bubble size distribution (ranging from hundreds of nanometers to tens of microns). From cro-SEM and TEM imaging it was shown that a self-assembled surfactant film coated the air/water interface. Thermodynamic and molecular models based on the energetic competition between the bending elasticity of the interface and the formation of domain boundaries were used to describe the pattern geometry. It was suggested that these features of the nano-scaling could be modified by changing the chemical composition of the film. Controlling the nature of the surfactant self-assembly could prove to be a useful tool in designing complex coatings to stabilize bubbles and foams. The structure of a neatly formed hexagonal surface pattern has been clearly demonstrated (41).

7.6.6   Hydrophobins

Biomolecules such as hydrophobins can outperform synthetic molecules in many applications, and there has been a growing interest in utilizing these natural polymers

in stabilizing bubbles and foams. These molecules are part of a class of small cysteine-rich surface-active proteins composed of amino acids, and they are commonly found in button mushroom. The structures contain distinctive hydrophobic and hydrophilic amino acid residues in the protein sequence and can be considered to have similar features to Janus particles. They form self-assemblies that are strong and irreversibly adsorb at the air/water interfaces, and they have been described as the most surface-active protein, known and produce surface tension reductions as low as 27 mN/m. In 2009, Cox and coworkers (42) showed that bubbles could be stabilized for long periods (for at least 4 months) and even up to several years in some cases.

The unique properties of hydrophobins have been reviewed by Linder (43) in 2009. Hydrophobins have also been evaluated as bubble stabilization agents in aerated foods such as ice cream, and early studies enabled them to be classified into two distinct groups: class I and II. In class I, aggregates form in water which are highly insoluble, whereas class II aggregates which are more soluble. On dispersion in water, class II produce oligomers which dissociate into aggregates and membranes that disintegrate when subject to shear deformation and transform into a viscoelastic layer similar to a highly elastic membrane. It is interesting to note that macroscopic bubbles formed in HFB II solution have been shown by Basheva and coworkers (44) to preserve the irregular non-spherical shape they had at the moment of solidification, as shown in Fig. 7.16.

There has been a considerable effort to understand the relationship between the functionality and the molecular rearrangements of the hydrophobin fragments, which
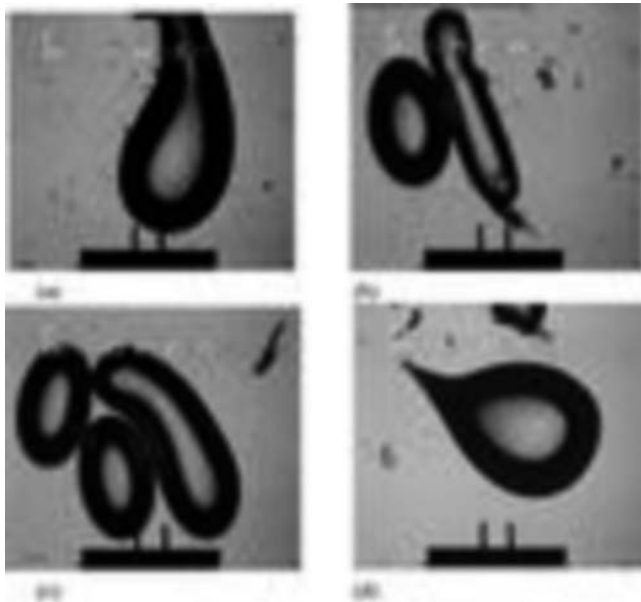

Fig. 7.16   Photograph of millimeter-sized bubbles resting below the surface of a 0.005 w% HFB class II solution containing added $CaCl_2$ (25 mM). From ref (44).

are produced under shear. Emphasis has been directed toward determining the size and geometry of the hydrophobic and hydrophilic head groups and the packing density at the interface. Basheva and coworkers (44) also carried out monolayer compression experiments and foam film studies which indicated that more mechanical, stiffer films were formed with hydrophobins than with more common proteins such as β-casein and β-lactoglobulin. These molecules appear to have sufficient hydrophobic and also hydrophilic moieties to form compact films with high packing densities, strongly attach to the bubble interface and reduce gas diffusion. They show periodic wrinkles (ripples) with well-defined bending elasticity. It has also been suggested that the protein monolayers of HFB II exhibited high mechanical strength compared to typical amphiphlic proteins. From free foam film studies, it was found that the interface was electrostatically stabilized, but near the pH_{iep}, aggregates were produced from dimers and tetramers that tended to adhere to each and to the air/water interface. Generally, these large aggregates in water could be considered to exhibit behavior similar to sticky particles, and this to some extent explains the compact adsorption layers. Also, it was suggested that expanding monolayers vulnerable to rupture could be repaired by the molecules filling the voids.

Adsorbed layers of hydrophobin HFB II with added β-casein were studied by Radulova and coworkers (45) using a rotational surface shear rheometer. Experiments were carried out at different shear rates and at different concentrations of added β-casein. High values of the surface shear elasticity were explained by the formation of an interfacial bilayer, with the layer from the more hydrophobic HFB II facing the air phase. With increase in shear rate, the layers were found to fluidize, and the addition of casein gave more rigid adsorption layers with faster fluidization. It was also possible to study the different processes that occur in the viscoelastic adsorption layer in different flow regimes which involve the breakage and restoration of intermolecular bonds and solidification of the adsorption layers. In Fig. 7.17, the results from surface rheological studies are shown together with a model illustrating the interfacial bilayer formed from the casein/HFB II aggregate.

7.6.7   Control of gas diffusion

Coherent interfacial films not only increase the surface elasticity but also have a major effect on the diffusion of gas across the aqueous films separating the bubbles. It is the structure of the thin film (the packing density, film type, the nature and concentration of the surfactant, molecular weight, the type of head group, electrolyte type and concentration, etc.) that plays a key role in defining the permeability of the barrier. In the case of polymers, thick layers are often adsorbed, but they are often porous due to the irregular alignments at the interface; however, they can become more effective when they become cross-linked after adsorption. Many proteins unfold at the interface, producing cross-linked layers, and some sucrose-based surfactants form crystallized defect-free dense films around the bubble. Although many studies have been carried out with proteins, the properties and composition of the adsorbed layers can change with aging, and also batch-to-batch variation occurs on storage, making it difficult to collect
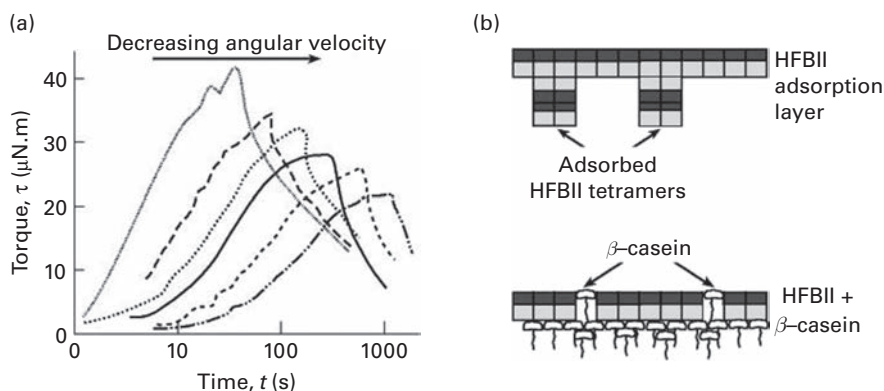
Fig. 7.17 Surface shear rheology studies on hydrophobin II: (a) plot of the torque versus time at six different angular velocities. The data indicate an increasing fluidization with rise in shear rate. (b) Top: HFB II dimers and tetramers can adhere to the film due to attractive interactions between hydrophilic parts of HFB II molecules. Bottom: With β-casein, an interfacial bilayer consisting of more hydrophobic HFB II facing the water phase and a layer of more hydrophobic casein that faces the water phase is formed. From ref (45).

reproducible experimental data on these systems. Particles can also jam on the bubble surface and become irreversibly adsorbed, and these layers can form effective barriers which decrease and even arrest the rate of bubble coarsening.

7.6.7.1 Gas type and foam type

The type of gas plays a key role in disproportionation since the permeation rate of the gas is proportionate to the gas solubility and the molecular size. For example, CO_2 gas is readily soluble in water (e.g. in soft drinks) and has 50 times greater solubility than N_2; this leads to less stable foams since the CO_2 is rapidly transported across the aqueous film. Gregorian and coworkers (46) generated foams for use in the textile industry with six different types of gases and found that the redistribution of bubble sizes for the different gases caused by disproportionation led to different rates of bubble growth and a decrease in foam bulk viscosity. Measuring the change in foam viscosity as a function of time enabled the stability of the foams to be estimated and the data are consistent with the hypothesis that the gas flow through the bubble walls occurs by an activated diffusion process.

A small fraction of relatively insoluble gas can effectively inhibit foam evolution and a binary gas mixture in which one of the gases is relatively insoluble can therefore be used to improve stability. In these systems, the disproportionation behavior becomes particularly interesting and as the gas composition of the bubble changes during shrinkage, the smaller bubbles become enriched by the lower solubility gas while the larger ones become enriched by the higher solubility gas. This effect is of practical importance in the brewing industry, where the addition of a low percent of N_2 to the CO_2 in beer is sufficient to stabilize the head of beer for some time after it has been drawn into a glass. Below a certain critical concentration of the insoluble gas, an inhomogeneous
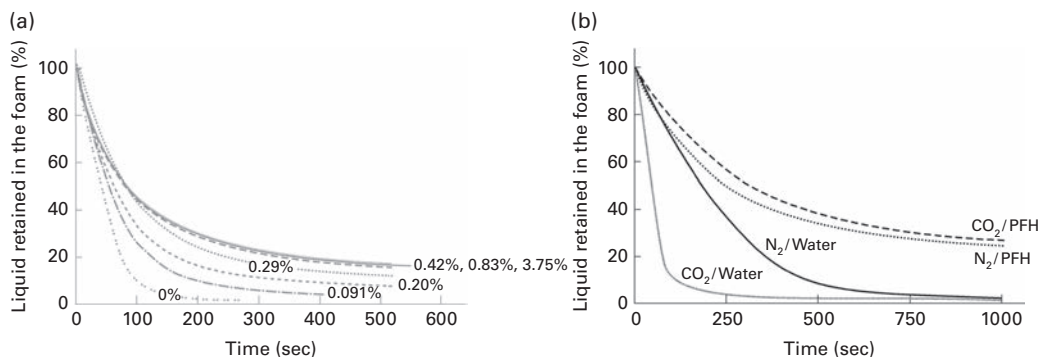
Fig. 7.18   (a) Drainage rates of foams produced from mixtures of CO_2 gas containing different concentrations of Perfluoro vapor. In this experiment FC104 vapor was selected. Solution contains 1 g/l of Pluronic F68. Initial volume of solution = 50 ml, temperature 25°C and rate of foam formation = 0.22 cm/s). (b) Comparison between two gases, CO_2 and N_2, with and without PFH solution. 1 g/l of Pluronic F68. V_0 = 50 ml, temperature 30°C and rate of foam formation = 0.22 cm/s. From ref (48).

structure is formed. This concept can be generally used to inhibit coarsening. For example, by bubbling a soluble gas through a small amount of liquid such as perfluor-ohexane (PFH), a small amount of insoluble vapor is introduced into the liquid causing the lifetime of a foam to be extended from only a few hours to several days. The theoretical background to this behavior has been presented by Weaire and cow-orkers (47) and is based on the differences in mixing entropies of the gas molecules which cause a counteractive driving force for gas diffusion.

The effectiveness of this method of stabilizing foams was evaluated in some detail in experiments by Gandolfo and Rosano (48) in which foams were generated in a column using a milk protein surfactant. Two systems were studied in which the stability of the foams (generated by N_2 and O_2) was measured from the changes in the drainage rates. Further experiments were made in which small concentrations of insoluble secondary gases (vapors) were introduced into these gases. Experiments were carried out with several different types of insoluble gases: Pluronic (F67: a block copolymer of ethylene oxide and propylene oxide condensate), a PFH and other types of commercial fluoro-inert (linear perfluoro molecules) designated FC 77, FC 104, FC 40 and FC 70. Fig. 7.18(a) shows a typical set of data of the drainage rates for foams generated by CO_2 containing increasing levels of the perfluoro vapor, compared to foams generated by bubbling CO_2 alone through the aqueous solution. The foams were generated at a fixed flow rate, and the gas supply was switched-off after the foam reached a pre-determined height.

These results show that an increase in the level of FC 104 in the gas mixture to above 0.42% caused the drainage curves to be reduced, and they finally level off. Also, in Fig. 7.18(b), the drainage results for CO_2 and N_2 are shown, and it can be seen that without the PFH vapor, the CO_2 causes a large increase in drainage rate compared with N_2, as expected. Nevertheless, it can be seen that by using gas mixtures containing PFH, the drainage can be substantially reduced for both gases.
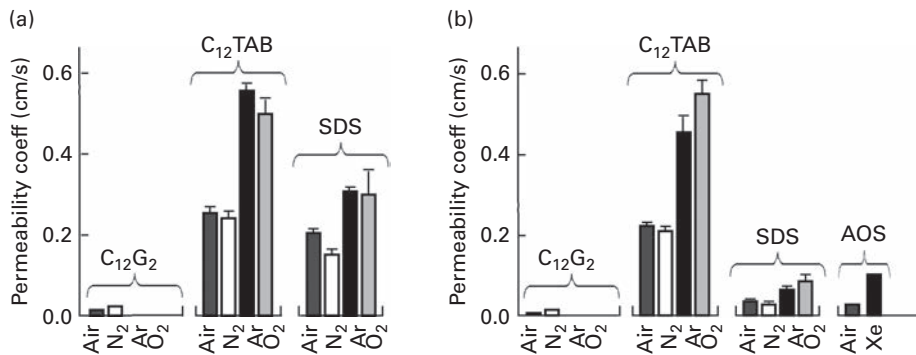
Fig. 7.19 Comparison of (a) gas permeability of CBF stabilized by β–$C_{12}G_2$, $C_{12}TAB$, SDS to different gases and (b) gas permeability of NBF stabilized by β – $C_{12}G_2$, $C_{12}TAB$, SDS and AOS to different gases. From ref (49).

Farajzdah and coworkers (49) measured the permeability rates (diffusion rates) of foam films prepared with anionic, cationic and nonionic surfactant solutions with several different types of gases which included argon, oxygen, nitrogen, air and in one case xenon. All the surfactant solutions were above the CMC, and the electrolyte concentrations were adjusted so that the film type could be changed. In the lower electrolyte concentrations, CBFs were formed with the ionic surfactants with typical equilibrium thicknesses of 10–15 nm, but at high electrolyte concentrations, NBFs were formed with thicknesses about 5 nm at 0.5 M electrolyte. The results of the gas diffusion experiments are summarized in Fig. 7.19 (a) and (b) for the two different film types, and this enables a comparison to be made between different surfactants, gases and types of film.

The results from this study indicate that the gas permeability of the CBFs were generally higher than that of the thinner NBFs, but this effect was mostly more pronounced for films stabilized by SDS surfactants. It is difficult to give a complete explanation of this behavior, but it is possible that the gas permeability is governed not only by the film thicknesses but also by the nature of the interacting surfactant monolayers, which would be dependent on the surfactant adsorption densities.

7.7 Interfacial rheology and gas permeability

There has been considerable debate on the influence of the surface elasticity on disproportionation. It has been thought that during this process, as small bubbles shrink, the film compacts and after a time the compression forces reach a sufficient magnitude to retard the shrinkage. However, it is possible that the adsorbed surfactant layers may collapse upon increasing compaction and form multilayers. A further possibility is that the molecules desorb from the surface. In 2008, Tcholakova and coworkers (50, 51) carried out a series of fundamental experiments using a mixed surfactant system in order to study the influence of gas permeability on interfacial rheology and drainage. Initially, a surfactant system was prepared by adding low
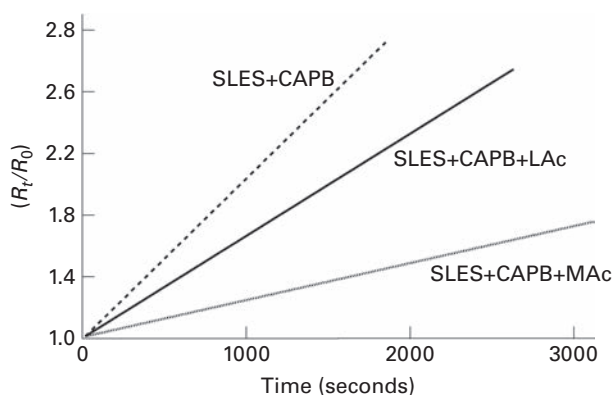
Fig. 7.20   Change of mean bubble radius R with time as a result of Oswald ripening. The bubbles are observed at the foam contact with a glass plate (the size of the first layer of bubbles was measured). From ref (50).

concentrations of a co-surfactant that was a medium-chain fatty acid, mystic acid (MAc) or lauric acid (LAc), to a mixture consisting of sodium lauryl–dioxyethylene sulfate (SLES) and a zwitterionic surfactant, cocamidopropyl betaine (CAPB) (50). Addition of the fatty acid surfactant to this mixture caused a substantial increase in dilational modulus which was explained by the formation of a surface-condensed phase of fatty acid molecules in the surface adsorption layer.

The permeability results obtained using the diminishing bubble experiments (which related the change in bubble size to time) are shown in Fig. 7.20, and these plots enable a comparison to be made of the different systems with and without the addition of the two fatty acids MAc and LAc.

These results indicate that the rate of diffusion was substantially reduced in the presence of the fatty acids, which exhibited a higher surface modulus, and the greater reduction occurred for the MAc. However, it was difficult to confirm that the rheological properties were playing a key role in retarding the gas diffusion, since the adsorbed fatty acid structured film alone would act as a barrier and reduce gas flow.

These initial studies were extended by Tcholakova and coworkers (51) using aminon L-02 Bis(2-hydroxyethyl)-lauramide as the added co-surfactants, instead of the fatty acids in order to give a low surface modulus. The permeability data again determined using both bulk foam experiments and the diminishing bubble method, and the results from the two methods gave good agreement. The results of the bubble shrinking process for the different systems indicated that the systems with high surface modulus tend to give slower rates of diffusion. However, Langmuir trough experiments indicated the surface tension of the shrinking and expanding bubble was low; this tended to suggest that interfacial elasticity did not play a major influence on the diffusion rate. An alternative mechanism was suggested to explain the decrease in gas diffusion which considered the formation of a surface-condensed phase (solid rather than fluid molecular packing) on the bubble surface, as illustrated in Fig. 7.21. This acted as a resistance to the diffusion of gas molecules across the film.
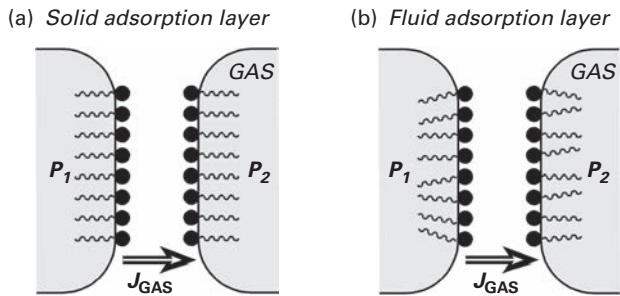
Fig. 7.21 Presentation of flux of dissolved gas across a foam film stabilized by surfactant with (a) high surface modulus and (b) low surface modulus. The formation of surface-condensed phase of surfactant molecules by myristic acid leads to a very low solubility and diffusivity of the dissolved gas molecules in the condensed adsorption layers on the foam film surface. From ref (51).
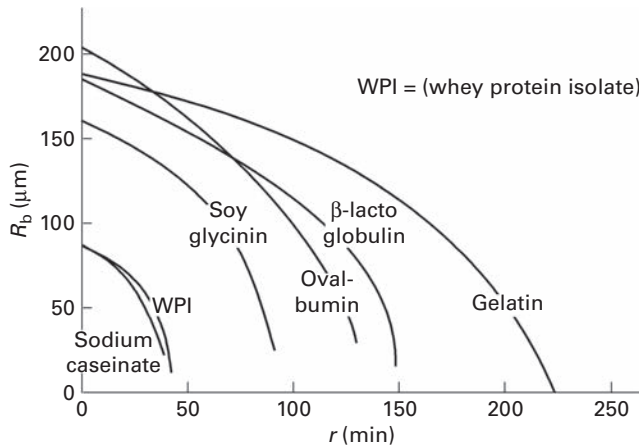

Fig. 7.22 Plot of bubble radius versus time for isolated bubbles near a planar air/water interface. Stabilized by different proteins at pH 7. From ref (52).

Dickenson and coworkers (52) concluded that irreversibly adsorbed globular proteins such as ovalbumin, which form highly viscoelastic films at the air/water interface, were capable of slowing down bubble shrinkage/expansion but not preventing it altogether. In this study, the rate of shrinkage of air bubbles beneath a planar air/water interface stabilized by four different types of proteins (whey protein isolate, sodium caseinate, gelatin, β-lactoglobulin) was measured, and it was found that fairly fast shrinkage of bubbles occurred in all cases, as shown in Fig. 7.22. Within one hour the bubble size was reduced to about 1 μm with no significant difference in rates. From the data, dilational modulus values were calculated for the proteins, and values ranged from 2.3 for gelatin to 12.5 mNm^{-1} for ovalbumin.

7.8   Stability by increase in bulk viscosity

Information on foam drainage rates is important in the design of many processes, particularly in the beverage and food industry and, as a general rule, the drainage rate of foams may be decreased by increasing the bulk viscosity of the liquid from which the foam is prepared. Overall, the more viscous the liquid, the slower is the downward flow of liquid between the bubbles. This may be achieved in aqueous systems by simply adding a solute such as glycerol, liquid paraffin or polyoxyethylene (high molecular weight (MW)) to the aqueous phase. Alternatively, the phase of the aqueous surfactant solution can be changed by adding electrolyte, thus producing a gel network. For many practical systems, such as food foams, the drainage can be easily halted by hydrous gel formation and the lamella stabilized at relatively large thicknesses (≈ 1 μm).

7.9   Stability control in aerated food systems

Although the basic framework for studying gas diffusion to the atmosphere from single bubbles is fairly well understood, there has been only limited work carried out to understand the gas diffusion in real aerated food systems. These usually consist of well-dispersed, high gas fraction systems with a large number of bubbles. In 2004, Dutta and coworkers (53) generated two aerated food products by whipping mesophase mixed dispersions (containing 33% sugar 65% water) with a 2% surfactant blend consisting of sucrose stearate together with either propylene glycol stearate (PPGS) or triglycerol stearate (TGS). The foams were allowed to stand, and the disproportionation process was evaluated by measuring the change in bubble size using video frames and microscopy. In addition, overrun, which was the decrease in the volume fraction of air in the foam, was measured. This could be considered as the difference in the degree of air lost to the atmosphere between the two systems due to the difference in diffusion rate in the two systems. The results are shown in Fig. 7.23(a) for the TGS-sucrose stearate system
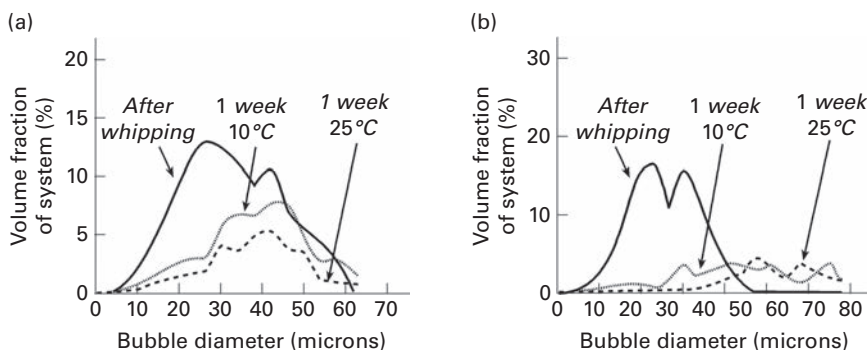

Fig. 7.23   The long-term stability of (a) triglycerol stearate surfactant system and (b) propylene glycol stearate surfactant system. From ref (53).

and in Fig. 7.23(b) for the PPGS-sucrose stearate system. These samples were prepared immediately after whipping and after a period of one week.

For the TGS system, the volume fraction did not change drastically after a week, whereas the PPGS was found to be more unstable. Also, the temperature of storage did not affect the size distribution to a great extent. The decrease in the overrun was explained by the diffusion of air from the bubbles to the atmosphere and was found to be higher at higher temperatures.

Two different types of models were developed to account for this behavior. The first model described the gas diffusion in terms of an inter-bubble diffusion occurring between bubbles of different sizes and driven by the difference in capillary pressure. The second model described the diffusion process in terms of the gas flowing from the larger bubbles to the atmosphere. Interestingly, the experimental results obtained from this study did not agree with the prediction of either models and it was necessary to construct a new gas diffusion model based on the combination of both models, which assumed that both processes occurred simultaneously. This combined diffusion model was found to give the most satisfactory fit to the experimental data.

7.10   Stratification

Johnnott (54) in 2006 and Perrin (55) in 1918 initially demonstrated that at surfactant concentrations beyond the CMC, organized molecular structures can be formed within thin films. This caused thinning of the film through a stepwise drainage mechanism known as stratification. It has been well established over the past 50 years that stratification can occur in dispersions of surfactant micelles, silica particles, microemulsions, globular proteins polymeric macromolecules and colloidal nanoparticles. Extended lifetimes have been observed for stratificating of liquid films, resulting in higher shelf-stability of foams. On thinning of the film, the particulates are forced into the restricted volume of the film which delays the drainage process and stabilises foam lamellae. The different steps in the drainage of the thin film containing a surfactant (above the CMC) are shown in Fig. 7.24(a) and for films containing low levels of surfactant in Fig. 7.24(b).

Organized structures can be formed from micelles produced from both ionic and nonionic surfactants in the aqueous solution and these provide an additional contribution to the disjoining pressure. These micelle layers flow out of the film to the Plateau borders, thus causing stepwise thinning, with each step corresponding to specific black spot concentrations (C_b). The phenomenon was earlier summarized by Ivan and Dimitrov (57), and several early experiments by Wasan and coworkers (58, 59, 60) showed that the ordering was caused by the interaction (via repulsive forces) of surfactant micelles or colloidal particles with narrow size distributions which were forced into the restricted volume of the film. These workers clearly showed that the ordered microstructure could play an important role in stabilizing foam lamellae. They suggested that the driving force for the stepwise thinning of the film was caused by the gradient of the chemical potential of the micelles at the film's periphery.
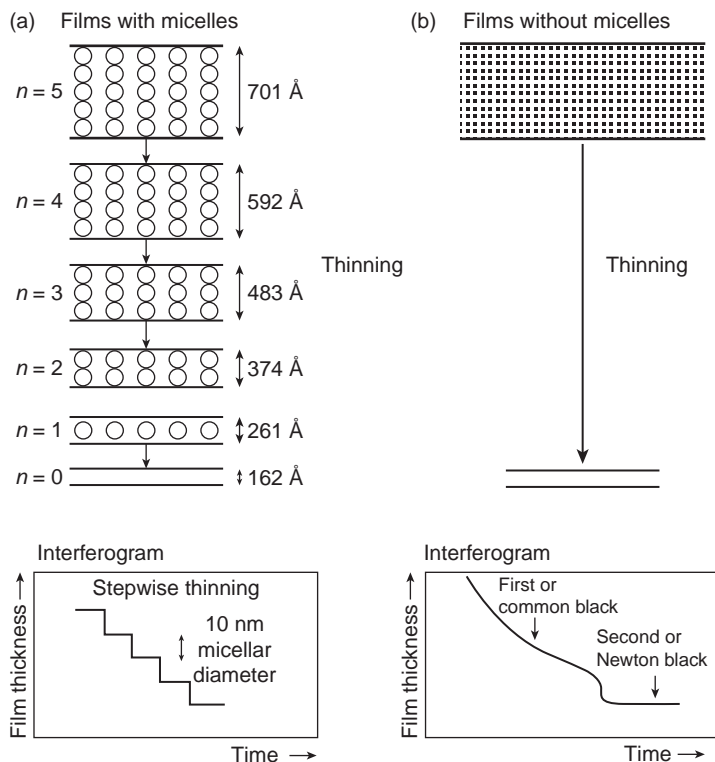
Both the experimental and theoretical aspects of these studies were summarized in 2007 by Wasan and Nikolov (61).

In 1992, Bergeron and Radke (62, 63) determined disjoining pressure isotherms for single isolated foam films stabilized by SDS at concentrations greater than the CMC. They reported that the oscillating component extended out to film thicknesses as large as 50 nm and that the discrete change in film thickness for each black film transition ranged from 6 to 10 nm and depended on the ionic strength and surfactant concentration. Studies of the oscillatory form of the disjoining pressure permitted quantitative interpretation of the stepwise thinning behavior.

7.10.1   Hole formation and the diffusion osmotic mechanism

In the stratified thinning process, the formation of a black spot in the film was considered to be associated with the dynamic removal of a layer of micellar species, which was considered to be initiated by the formation of a hole and subsequent sheeting of a hole which occurs at each step. Bergeron and coworkers (64) developed a nonlinear hydrodynamic stability analysis that modeled the dynamics of the hole formation and
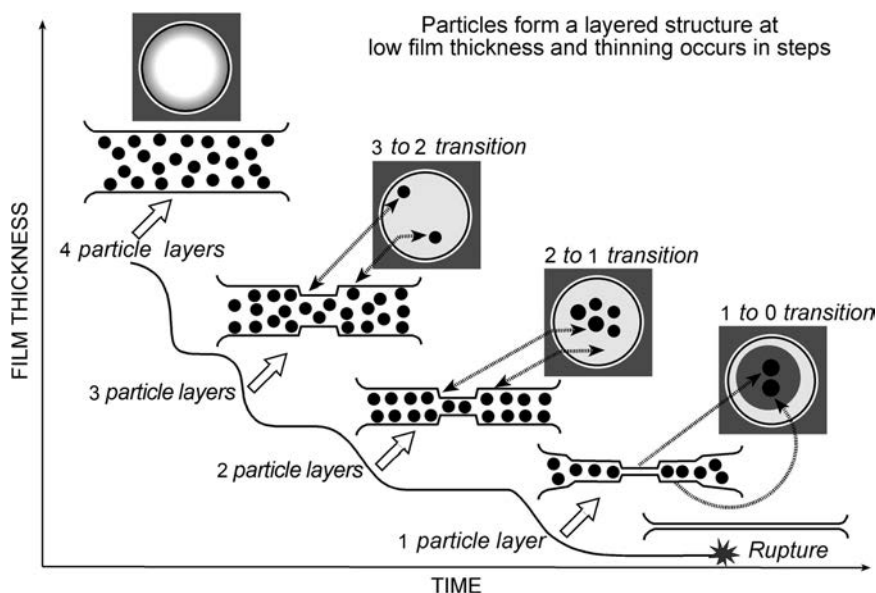
Fig. 7.25 The layer-by-layer thinning of the micellar films is triggered by the formation of black spots inside the film. One can distinguish up to five stratified layers shown by photocurrent time plot. From ref (65).

sheeting by taking into account an equilibrium oscillating structured component of the disjoining pressure. They attributed the initiation of a hole in the film to the nonlinear growth of hydrodynamic instability that occurred under the action of a constant capillary pressure and oscillating disjoining pressure. The subsequent growth of the hole was explained by the outward fluid flow within the inhomogeneous thin film as radial pressure gradients developed from curvature variations and viscous resistance to flow. In the final stage, a small black spot appears in the film which contained only one layer of particles and continues to expand until the film ruptures. The black spot expands because the particles leave the films and the expansion rate can be used as a measure of exodus from film. The complete thinning process that occurs through stepwise transitions is summarized in Fig. 7.25.

The black spot expansion during the last transition was found to be dependent on film size and it was found that the area of black spot expanded linearly with time. A vacancy diffusion osmotic (DO) mechanism of film thinning was proposed by Kralchevsky and coworkers (59). In this theory, the thickness transformation from h_n to h_{n-1}, where n is the number of micellar layers, occurs due to the decrease in free energy, and it was assumed the film thickness transition was in a metastable state. The process of the micelles leaving the film at each step resulted from the osmotic pressure gradient and involves the provision of vacancies by a condensation mechanism controlled by the film size for a fixed micellar concentration. However, although this theory has been used to account for the stratification of SDS and CTAB micellar solutions and also for charged
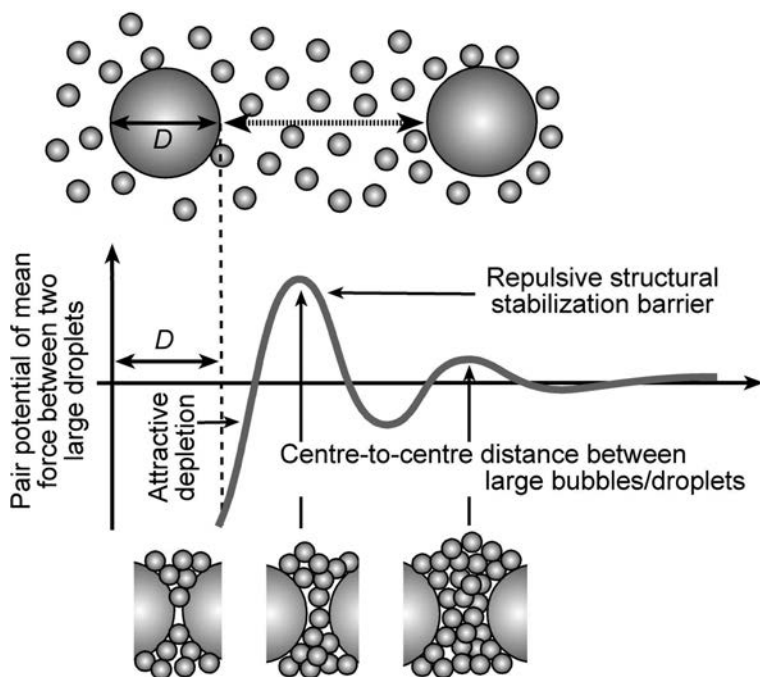
Fig. 7.26   Interdroplet interactions and resulting oscillating structural forces within the thin liquid film separating the bubbles. Both attraction depletion forces and structural barriers occur between bubbles. From ref (69).

particles, it does not fit the nonionics where the transition is a reversible process. In fact, for the nonionics, the energy of both stable states must be almost identical.

Several theoretical models have been developed over the years by Wasan and co-workers (66, 67, 68, 69, 70, 71) during the period 2001–2004 to rationalize the experimental results. Generally, the oscillation component comprised an attractive depletion component opposing the repulsive structural energy barrier inside the film. In the case of very thin intervening film when the thickness is less than the micellar size, the micelles became excluded from the film, and osmotic pressure inside the film is reduced. This causes an attractive depletion force (i.e. Asakura–Osawa depletion attraction). However, when the film thickness is of the order of several micellar diameters, the micelles are ordered in the confines of the film surfaces, thereby resulting in a structural energy barrier separating (stabilizing) the bubbles (Fig. 7.26).

Further studies were carried out based on statistical mechanics, and numerical Monte Carlo simulations have been performed using an effective one-component fluid potential model that incorporated particle hard-core repulsion. Both the screened Coulombic electrostatic interaction and the entropic contribution due to the discrete nature of the solvent and the finite size of the electrolyte ions were included in these models. Concise formalism was developed based on the generalization of Ornstein–Zernike equations for fluid mixtures, and it was found that in hard-sphere colloidal suspension, comprised of larger entities, the solvent molecules

enhance the structural forces both among the larger particles themselves and between them and the film interfaces (68, 69, 70).

7.10.2   Reversible stratification behavior in nonionic surfactants

Stratification is well known to be an important mechanism for many nonionic foams. Niskolov and Wasan and coworkers (69) carried out stratification experiments using curved and flat films which were stabilized by nonionic ethoxylated alcohols (containing 15–16 n-carbons chain length and 13 ethylene oxide groups). Experiments were carried out at three concentrations: 2, 4 and 8% corresponding to 3.25, 6.50 and 13.00 times CMC. The capillary force balance apparatus was used in conjunction with combined differential and common interferometric methods, and this enabled the film curvature, film radius, capillary pressure and film thickness to be monitored simultaneously. In addition, the effect of film size on the lamella thickness transition was investigated. In Fig. 7.27(a) and (b), the stratification is shown for micellar film made from surfactant concentration at 3.25 CMC, with two films of different sizes.

With the smaller film (diameter 17.5 micron and surface area 2.6×10^{-4} cm^2) as shown in Fig. 7.27(a), two stepwise thickness transitions were observed, one at a thicknesses of 42.7 nm and one at a thickness of 33.2 nm; the amplitude of thickness transition is about 9 nm which is equal to an effective micelle diameter. After these two thickness transitions, the film remains stable at 25 nm with one micellar layer inside it. However, at the greater film diameter (250 microns with area of 5.9×10^{-4} cm^2 and a capillary pressure of 38.5 Pa) as shown in Fig. 7.27(b), one more stepwise thickness is observed. It was also observed that as the film thickness decreases, the time for the next thickness stepwise transition to occur increases and also that the stepwise transition occurs more rapidly for the

(a)
Film area: $S = 2.6\ 10^{-4}$ cm^2
Capillary pressure: 40.7 Pa

Photocurrent (film thickness)

42.7 nm
33.2 nm
25.0 nm

Time (min)

(b)
Film area: $S = 5.9\ 10^{-4}$ cm^2
Capillary pressure: 38.5 Pa

Photocurrent (film thickness)

42.7 nm
33.2 nm
25.0 nm
17.0 nm

Time (min)

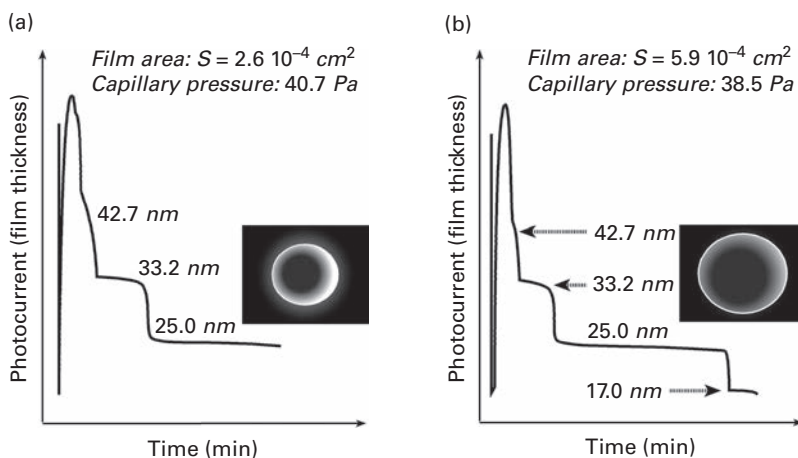**Fig. 7.27**   Photocurrent versus interferogram of the thinning of a curved foam film at a surfactant concentration of 2% (3.25 × CMC) depecting the effect of film size on film stepwise thinning. Film areas (a) 2.6 x 10^{-4} and (b) 5.9 x 10^{-4} cm^2. From ref (67, 69).

larger film. In addition, it was observed that when the thickness is reduced from 250 to 175 microns, the film slowly increases in thickness from 17 back to 25 nm (from one micellar layer to two micellar layers), indicating that micellar lamellar layer thinning occurred as a reversible process. This unusual thinning behavior of micellar nonionic films could not be explained by the previously proposed diffusive-osmotic mechanism which had been successfully applied to anionic or cationic micellar films. For charged ionic surfactants, the formation of black spots in micellar films was based on a micellar vacancy diffusive-osmotic mechanism, which assumed that the film at each stepwise transition is in a metastable state. In fact, for the nonionics, the energy of both stable states must be almost same.

Generally, it was concluded from these studies that the stability of the micellar films is governed by the film size (the bubble size), and the capillary pressure but the concept of disjoining pressure isotherm alone cannot predict film thickness stability. Experiments show that film stability depends more on the lamella or film size and micelle concentration and less on the capillary pressure.

7.10.3   Stratification in charged surfactant systems

In the case of foam films formed from micellar solutions of nonionic surfactants (uncharged micelles), the height of the stratification layer ($h_1 - h_2 = \Delta h$) was considered to be equal to the diameter of a hard sphere but slightly decreasing with the rise of the particle volume fraction. However, with ionic micelles, the step height is greater than the micelle hydrodynamic diameter, and it is accepted that another double-layer thickness counterion atmosphere needs to be considered in estimating the thickness. Electrostatic interaction between charged micelles plays a key role during the thinning process.

Although this is a physically correct interpretation, a more detailed model was developed by Danev and coworkers (72) for charged surfactant systems in which the step height and final thickness of the film was related to the micelle size. Initially, these workers carried out stepwise stratification experiments using a Schedudko Exerowa cell (see Chapter 3) for an anionic and two cationic surfactant systems (SDS CTAB and cetyl pyridinium chloride (CPC)) at concentrations above the CMC. From the results, both values of step height and final thickness of the films could be related to the bulk surfactant concentrations for the three systems. The step heights were found to be equal: $h_3 - h_2 = h_1 - h_0 = \Delta h$ which enabled data to be collected in which Δh and h_0 could be related to the surfactant concentration. Theoretical models could then be constructed to interpret this dependency. Two approaches were considered; first an energy approach where the step height was identified with the effective diameter of charged micelle. The charge on films and micelles was calculated using a charge regulation model. Also, a second approach was attempted based on osmotic pressure in which the step height was dependent on the number density of the micelles in bulk solution.

With regard to the distribution of micelles in the systems, three models were tested: a Poisson–Boltzmann model, a Jellium approximation (JA), which assumes a uniform

charge distribution, and a cell model. The JA model assumes that micelle concentration was uniformly distributed, despite the field of electric double layers. It was found that the JA gave the best agreement between theory and experiment. In fact, two theoretical approaches which were based on energy and osmotic pressure were found to give reasonable agreement. The experimental data providing the suspension of charged micelles was represented as Jellium. This model proved to be useful for determining the aggregate number of ionic surfactant micelle from the experimental heights of the steps. It was also concluded from theory (based on the dispersion of charged particles behaving as jellium) and experiment that the thinnest stable films (h_0) experimentally observed were thick enough to contain micelles (at very low concentration) to ensure the osmotic balance between the film and bulk solution.

7.10.4 Stratification in polydispersed systems

In many practical industrial systems, the particles are rarely monodispersed, and Wasan and coworkers (65, 73) have shown from experiments and calculations that the poly-dispersity has a pronounced effect on stratification and film stability and can cause a weakening effect on the particle layering (structural barrier) and a reduction of foaminess. Stratification experiments were carried out with bidispersed mixtures pre-pared from of mono-dispersed particles (8% v/v of 8 nm sized hydrophilic colloidal silica particles with an addition of 2% v/v of 100 nm particles). The effective volume fraction of particles was about 0.35. Initially, stratification experiments were carried out using films of different sizes (diameters 133 and 105 μm) for these bidispersed systems, and the change in size of the black spot expansion rate of the last transition was recorded (Fig. 7.28). These plots show that black spot expansion rate and area expand linearly
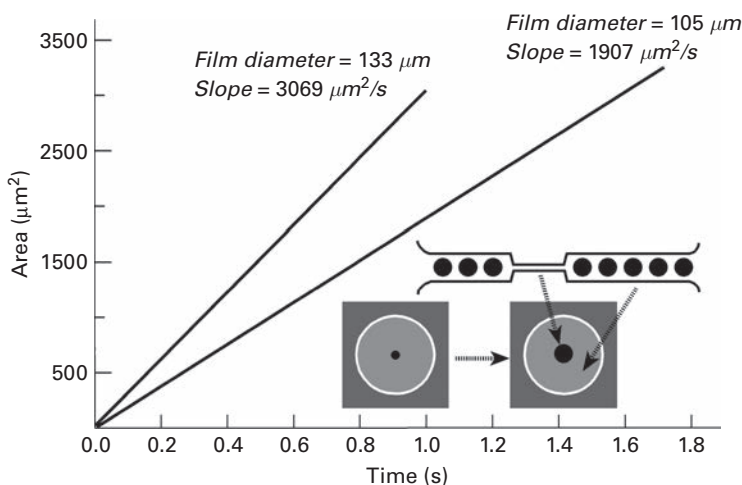

Fig 7.28 Black spot expansion bidispersed mixtures at different film sizes. From ref (63).
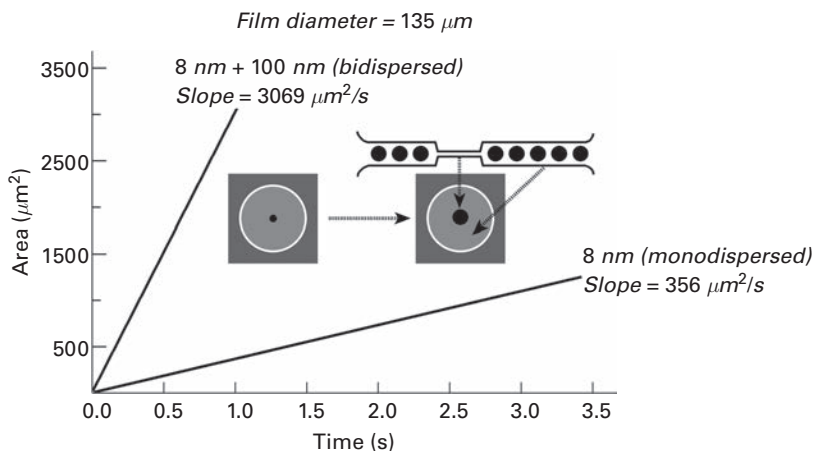
Fig. 7.29   Black spot expansion for monodispersed and bidispersed cases at comparable film sizes. From ref (63).

with time for both systems, but rate of expansion of the bidispersed systems was the greatest for the large film sizes.

In a second series of experiments, the spot expansion rate for monodispersed system was compared with a bidispersed system for films of about the same diameter (135 microns), and the results are shown in Fig. 7.29. In this case, it can be seen that the monodispersed particles and the bidispersed particles left the film more rapidly. Generally, it was concluded from these studies that the rate of particle movement from the film to the bulk was the lowest for the monodispersed system, intermediate for the polydispersed (prepared by mixing three different sized particles) and the highest for the bidispersed system, and in general, monodispersed particles exhibit slower expulsion and more stable films. However, in case of the experiments in curved and plain films, an increased particle efflux from the film to the meniscus was reported for the polydispersed systems. It was also found that the black spot area expands linearly with time and the larger films exhibit faster rates of spot expansion which was explained by the DO model. The influence of polydispersity on the structure barrier oscillation and oscillation forces was discussed by Wasan and coworkers (65), and a representative picture of the interaction is shown in Fig. 7.30.

It was stressed that confined in-layer structures in films were essential for retarding thinning and that polydispersity leads to the weakening of particle laying (decreasing in the structural barrier) and film stability. But, in addition, it is the degree of polydispersity that plays an important role in the height of the energy barrier. The interactions between two approaching bubbles in a polydispersed system are shown in Fig. 7.30(a), where initially a weak barrier (Us) is encountered but on further thinning smaller particles are ejected from the film (Fig. 7.30(b)). This results in a reduction in polydispersity and an improvement in layer structuring which causes the height of the structural barrier to increase. However, on reaching a critical thickness the particles are finally ejected and a depletion well is encountered. In Fig. 7.30(c), the relationship
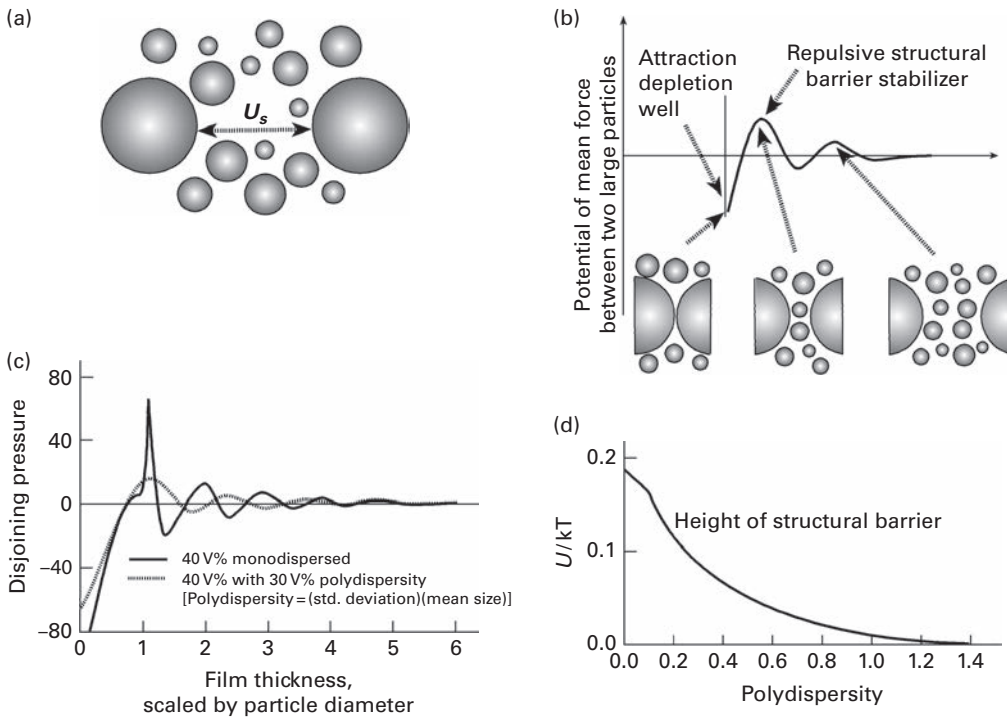
Fig. 7.30 Effect of particle polydispersity on the height of the structural barrier between film surfaces. From ref (63).

between film thickness and the disjoining pressure is illustrated for a monodispersed and polydispersed system. In both cases, the oscillating disjoining pressure is increased as the film thickness is reduced for both systems. The height of the barrier is a measure of the film stabilizing effect, and in Fig. 7.30(d), it is related to the degree of polydispersity.

7.11 Stabilization by liquid crystals

It is well known that liquid crystals can adsorb at the bubble interface and stabilize both aqueous and non-aqueous foam systems. At higher surfactant concentrations, the liquid crystalline surface phase is often in equilibrium with a bulk isotropic phase. The stability in non-aqueous systems is covered in Chapter 9. Frequently, liquid crystals have been formed in aqueous mixed surfactant systems, for example, by the addition of small amounts of a nonionic surfactant to an anionic surfactant, which can lead to enhanced foam stability. In addition, there are several possible explanations to account for the increase in foam stability caused by the precipitation or formation of crystalline or structural aggregates in the solution. For example, they may cause a reduction in hydrodynamic drainage or retardation in interfacial drainage caused by viscous layers or an increase in the mechanical
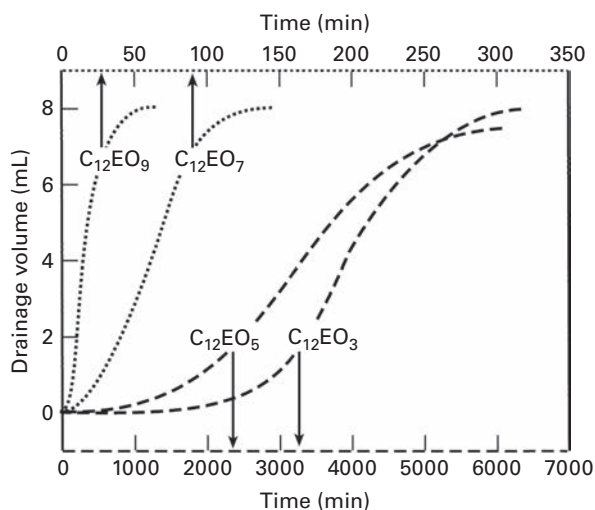
Fig. 7.31   Liquid drainage from foams stabilized solely by C_{12} E_n type surfactant (30wt%). From ref (77).

strength of a liquid film, which may increase the resistance between bubbles. Also, the accumulation of the liquid crystal phase in the lamellae film may reduce the diffusion rate of entrapped gas. In addition, there is a possibility that accumulation in Plateau borders can distort the radius of curvature which may influence the Laplace pressure. Although the liquid crystals may act as a reservoir of surfactant, they are unlikely to enhance the Gibbs–Marangoni elasticity since early studies have indicated that the dispersed liquid crystalline phase, rather than micelles, exhibits the diminished rates of transport to the bubble interface. This would suggest that relatively low levels of dynamic adsorption would lead to a lowering of foamability (74).

Novales and coworkers (75) in 2010 carried out foaming studies on fatty acid–lysine salts in aqueous solution. The alkyl chain length was varied from dodecyl to stearic and an attempt was made to relate the foamability to the phase behavior. Extremely stable foams were obtained with palmitic acid/lysine salts, but for other chain alkyl length poor foams or no foaming was reported. It was found that the structural aggregates played an important role in foaming, and quantitative information on the aggregate structure could be obtained using a transmission electron microscope, differential scanning calorimetry, solid state NMR and small-angle neutron scattering. In aqueous solution, the lysine salt of the dodecyl chain gave an isotropic micellar solution, whereas for longer alkyl chains, the fatty acid vesicles were embedded in a lamellar arrangement that passes from gel to fluid state on aging or upon heating. At low concentration no significant structure has been detected.

Shrestha and coworkers (76) in 2006 studied the foaming characteristics of penta-glycerol monostearate ($C_{18}G_5$) and penta-glycerol monoleate ($C_{18:1}G_5$) in dilute aqueous solution. Both surfactants showed an increase in foaming with

concentration and foams prepared from $C_{18}{:}1G_5$ shown to be less stable than foam prepared from $C_{18}G_5$. Also, dispersions of α particles and L_α phase could be detected in the water-rich regions for both systems but, it was not possible to explain this difference in foaming, and no correlation between dynamic interfacial properties and foaming could be established. Chen and coworkers (77) showed that the stability of foams produced from the series of low molecular weight polyoxyethylene-type nonionic surfactants ($C_{12}EO_n$) could also be explained by the formation of liquid crystals. In these experiments, the foam stability was evaluated from the drainage profiles (the volume of liquid drained plotted as a function of time). A wide range of profiles was detected, and the stability initially increased with increments of concentration for each nonionic. It was found that maximum foamability occurred at 10 w% except for $C_{12}EO_n$ which occurred at 1 wt%. In Fig. 7.31, the drainage volumes of foams stabilized by the different nonionic surfactants in the series $C_{12}E_n$ are shown corresponding to 30 w% surfactant concentration. "S"-shaped profiles are shown and three stages in the drainage curves were identified: an initial stable stage, followed by a rapid gravity-driven liquid drainage region which accounted for removal of 90% of the liquid and the final thinning of the foam films.

The viscosities and microstructures were also explored; for $C_{12}EO_3$ and $C_{12}EO_5$ the maximum stability occurred at 30 wt% structures, which was explained by the presence of high concentrations of lamellar liquid crystals adsorbed at the interface. These were clearly visible between bubbles, and the foams and were stable for about 20 hours. In the case of $C_{12}EO_7$ and $C_{12}EO_9$ the stability was considerably lower; it was only for 10 minutes and no liquid crystals were detected.

7.12 Stabilization by emulsion and pseudo-emulsion films

Wasan and coworkers (78) investigated the influence of oil (in the micellar environment) on the stability of foam. Two different types of emulsified oil systems were studied which consisted of (a) a microemulsion (solubilized within the micelle) and (b) a macroemulsion. It was found that in each case the foam stability was affected by a completely different mechanism. In the first case, where the foam film containing oil, it solubilized within the micelle to form a microemulsion and the normal micellar interactions are changed. It had been earlier demonstrated that micellar structuring causes stepwise thinning due to layer-by-layer expulsion of micelles and that this effect was found to inhibit drainage and increase the foam stability. Generally, this stratification phenomenon was found to be inhibited by the oil solubilized within the micelle, which decreased the micelle volume (representing a decrease in the repulsion between the micelles). In the case of the macroemulsified oil system, the important role of the so-called pseudo-emulsion film (formed between the air/water interface and an approaching oil droplet) in the stability of the aqueous foaming system was emphasized (Fig. 7.32).
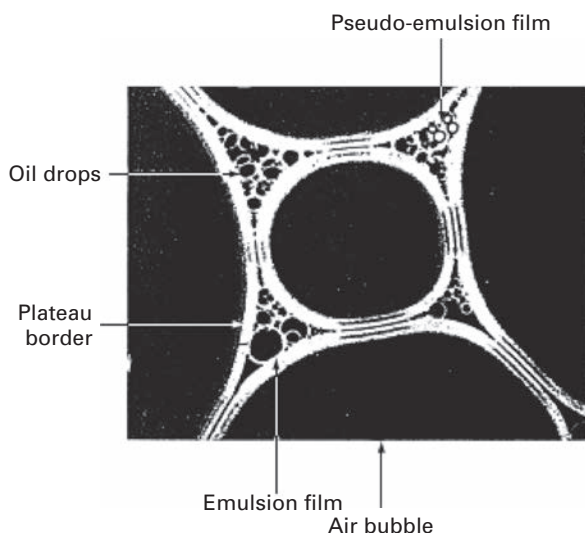
Fig. 7.32   Illustration of a macroemulsified oil system. The drainage of the film may be reduced due to accumulation of emulsified oil droplets within the Plateau borders. The formation of the emulsion film and pseudo-emulsion film are indicated. Factors affecting the foam stability were found to be oil volume fraction, drop size and oil phase density.

References

(1) B. P. Binks, R. Murakami, S. P. Armes, S. Fujii and A. Schmid, pH Responsive Aqueous Foams Stabilized by Ionized Latex Particles, *Langmuir*, **23**, 8691–8694, 2007.

(2) K. Engelhardt, A. Rumpel, J. Walter, J. Dombrowaki, U. Kulozik, B. Braunschweig and W. Peukert, Protein Adsorption at the Electrified Air-Water Interface: Implications on Foam Stability, *Langmuir*, **28**, 7780–7787, 2012.

(3) A. P. J. Middelberg and M. Dimitrijev-Dwyer, A Designed Biosurfactant Protein for Switchable Foam Control, *ChemPhyschem*, **12**, 1426–1429, 2011.

(4) A.-L. Fameau and coworkers, Smart Foams: Switching Reversibly between Ultrastable and Unstable, *Angew. Chem. Int. Ed.*, **50** (36), 8264–8269, 2011.

(5) A.-L. Fameau, S. Lam and O. D. Velev, Multi-Stimulus Responsive Foam Combining Particles and Self-Assembling Fatty acids, *Chem. Sci.*, **4**, 3874–3881, 2013.

(6) H. Lu, Y. He and Z. Huang, Foaming Properties of CO_2-Triggered Surfactants for Switchable Foam Control, *J. Dispersion Sci. Technol.*, **35**, 832–839, 2014.

(7) J. Lucassen, Longitudinal Capillary Waves. Part 1. Theory, *Trans. Farad. Soc.*, **64**, 2221–2229, Part 2, Experimental 2230–2235, 1968.

(8) I. B. Ivanov, K. D. Danov, K. P. Anathapadmanabhan and A. Lips, Interfacial Rheology of Adsorbed Layers with Surface Reaction: On the Origin of the Dilational Surface Viscosity, *Adv. Colloid Interface Sci.*, **114**–115, 61–92, 2005.

(9) M. A. Bos and T. van Vliet, Interfacial Rheological Properties of Adsorbed Protein Layers and Surfactants: A Review, *Adv. Colloid Interface Sci.*, **91**, 437–471, 2001.

(10) M. van den Temple and R. P. van de Riet, Damping of Waves by Surface Active Materials, *J. Chem. Phys.*, **42**, 2769–2769, 1965.

(11) K. D. Wantke, H. Fruhner, J. Fang and K. Lunkenheimer, Measurements of the Surface Elasticity in Medium Frequency Range Using the Oscillating Bubble Method, *J. Colloid Interface Sci.*, **208**, 34–38, 1998.

(12) R. Miller and L. Liggieri, Eds., *Interfacial Rheology, Progress in Colloid and Interface Science, Series*, Brill Publishers, Leiden, Boston, 2009; L. Liggieri and R. Miller, Relaxation of Surfactants Adsorption Layers at Liquid Interfaces, *Curr. Opin. Colloid Interface Sci.*, **15**, 256–265, 2010.

(13) S. R. Derkash, J. Kragel and R. Miller, Methods of Measuring Rheological Properties of Interfacial Layers (Experimental Methods of 2D Rheology), *Colloid J.*, **71** (1), 1–17, 2009.

(14) J. Ding, H. E. Warriner, J. A. Zasadzinski and D. K. Schwartz, Magnetic Needle Viscometer for Langmuir Monolayers, *Langmuir*, **18**, 2800–2806, 2002.

(15) S. Reynaert, C. F. Brooks and P. Moldenaers, Analysis of the Magnetic Rod Interfacial Stress Rheometer, *J. Rheol.*, **52**, 261–286, 2008.

(16) G. Kretzschmar and K. Lunkenheimer, Studies for Determination of Elasticity of Adsorption Films of Soluble Surface Active Substances, *Ber. Bunsenges. Phys. Chem.*, **74**, 1064, 1970.

(17) K. D. Wantke and H. Fruhner, Determination of the Surface Dilational Viscosity Using the Oscillating Bubble Method, *J. Colloid Interface Sci.*, **237**, 185–199, 2001.

(18) F. Ravera, G. Loglio and V. I. Kovalchuk, Interfacial Dilational Rheology by Oscillating Bubble/Drop Methods, *Curr. Opin. Colloid Interface Sci.*, **15**, 217–228, 2010.

(19) R. Miller and L. Liggieri, Surface Rheology as a Tool for the Investigation of Processes Internal to Surfactant Adsorption Layers, Disc. *Faraday Soc.*, **129**, 125, 2005.

(20) L. Liggieri, and coworkers, Eds., *Drops and Bubbles in Interfacial Research*, Vol. **6**, 239–278, Elsevier, 1998.

(21) S. Hard and R. D. Neuman, Laser Light Scattering Measurements of Viscoelastic Monolayer Films, *J. Colloid Interface Sci.*, **83**, 315–338, 1981.

(22) D. M. Colegate and C. D. Bain, Adsorption Kinetics in Micellar Solutions of Nonionic Surfactants, *Phys. Rev. Lett.*, **95**, 198302, 2005.

(23) K.-D. Wantke, H Fruhner and J. Ortegren, *Colloids Surf., A*, **221**, 185–195, 2003.

(24) A. Anderson and coworkers, Oscillating Bubble SHG on Surface Elastic and Surface Viscoelastic Systems; New Insight in the Dynamics of the Adsorption Layers, *J. Phys. Chem. B*, **110**, 18466–18472, 2006.

(25) N. Schelero, G. Hedicke, P. Linse and R. V. Klitzing, Effect of Counterions and Co-ions on Foam Films Stabilized by Anionic Dodecyl Sulphate, *J. Phys. Chem. B*, **114**, 15523–15529, 2010.

(26) M. J. Schick and I. R. Schmolka, In *Nonionic Surfactants Physical Chemistry*, Ed. M. J. Schink, Marcel Dekker, New York, 1987.

(27) M. J. Schick and F. M Fowkes, Foam Stabilizing Additives for Synthetic Detergents: Interaction of Additives and Detergents in Mixed Micelles, *J. Phys. Chem.*, **61**, 1062–1068, 1957.

(28) H. L. Sanders and E. A. Knaggs, Foams Stabilized by Alkloamides in Shampoos, *Soap Sanitary Chem*, **45**, 1953.

(29) C. Rodriguez, T. Sakai, R. Fujiyama and H. Kunieda, Phase Diagrams and Microstructure of Aggregates in Mixed Ionic Surfactant/Foam Booster Systems, *J. Colloid Interface Sci.*, **270**, 483–489, 2004.

(30) E. S. Basheva and coworkers, Role of Betaine as a Foam Booster in the Presence of Silicone Oil, *Langmuir*, **16** (3), 1000–1013, 2000; Foam Boosting by Amphiphilic Molecules in the Presence of Silicone Oil, Langmuir, *Langmuir*, **17**, 969–979, 2001.

(31) K. Holmberg, B. Jonsson, B. Kronberg and B. Lindman, Eds. *Surfactants and Polymers in Aqueous Solution*, John Wiley and Sons, New York, 1998.

(32) R. V. Klitzing and H.-J. Muller, Film Stability Control, *Curr. Top. Colloid and Interfacial Science*, **7**, 42–49, 2002.

(33) D. Langevin, Polyelectrolytes and Surfactant Mixed Solutions Behaviour at Surfaces and in Thin Films, *Adv. Colloid Interface Sci.*, **89**–90, 467–484, 2001.

(34) M. M. Guerrini, R. Y. Lochhead and W. H. Daly, Interactions of Aminoalkylcarbanoyl Cellulose Derivatives and SDS, 2. Foam Stabilization, *Colloids Surf., A*, **147**, 67–78, 1999.

(35) J. Djuve, R. J. Pugh and J. Sjoblom, Foaming and Dynamic Surface Tension of Aqueous Polymer/Surfactant Solutions, 1. Ethyl (hydroxyl Ethyl) Cellulose and Sodium Dodecyl Sulphate, *Colloids Surf., A*, **186**, 189–202, 2001.

(36) D. Langevin, C. Marquez-Beltran and J. Delacotte, Surface Force Measurements on Freely Suspended Liquid Films, *Adv. Colloid Interface Sci.*, **168**, 124–134. 2011.

(37) V. Bergeron, D. Langevin and A. Asnacios, Thin Film Forces in Foam Films Containing Anionic Polyelectrolyte and Charged Surfactants, *Langmuir* **12** (6), 1550–1556, 1996.

(38) A. Saint-Jalmes, M. L. Peugeot, H. Ferraz and D. Langevin, Differences between Protein and Surfactant Foams: Microscopic Properties, Stability and Coarsening, *Colloids Surf., A*, **263** (1–3), 219–225, 2005.

(39) N. Schelero and R. von Klitzing, Effects of Oppositely Charged Surfactants on the Stability of Foam Films, *Colloids Surf., A*, **382**, 165–173, 2011.

(40) Y. Shen, R. L. Powell and M. L. Longo, Interfacial and Stability Study of Microbubbles Coated with a Monostearin/Monopalmitin-Rich Food Emulsifier and PEG40 Stearate, *J. Colloid Interface Sci.*, **321**, 186–194, 2008.

(41) E. Dressaire, R. Bee, D. C. Bell, A. Lips and H. A. Stone, Interfacial Polygonal Nano-patterning of Stable Microbubbles, *Science*, **320**, 1198–1200, 2008.

(42) A. R. Cox, D. L. Aldred and A. B Russell, Exceptional Stability of Food Foams Using Class II Hydrophobin (HFB II), *Food Hydrocolloids*, **23**, 366–376, 2009.

(43) M. B. Linder, Hydrophobins: Proteins that Self-Assemble at Interfaces *Curr. Opin. Colloid Interface Sci.*, **14**, 356–363, 2009.

(44) E. S. Basheva and coworkers, Unique Properties of Bubbles and Foams Films Stabilized by HFBII Hydrophobin, *Langmuir*, **27**, 2382–2392, 2011.

(45) G. M. Radulova and coworkers, Surface Shear Rheology of Adsorption Layers from Protein HFBII Hydrophobins: Effect of Added Beta-Casein, *Langmuir*, **28**, 4168–4177, 2012.

(46) R. Gregorian, R. Bafford and M. Duke, Influence of Foaming Gas on Foam Stability, *Tex. Res. J.*, **53**, 267–270, May 1983.

(47) D. Weaire and V. Pageron, Evolution of Foam Inhibited by an Insoluble Gaseous Compound, *Philos*, *Mag. Let.*, **62**, 417–421, 1990.

(48) F. G. Gandolfo and H. L. Rosano, Interbubble Gas Diffusion and the Stability of Foams, *J. Colloid Interface Sci.*, **194**, 31–36, 1997.

(49) R. Farajzdeh and coworkers, Effect of Gas Type of Foam Film Permeability and Its Implications for Foam Flow in Porous Media, *Adv. Colloid Interface Sci.*, **168**, 71–78, 2011.

(50) K. Golemanov, N. D. Denkov, S. Tcholakova and M. Vethamuthu, A. Lips Surfactant Mixtures for Control of Bubble Surface Mobility in Foam Studies, *Langmuir*, **24**, 9956–9961, 2008.

(51) S. Tcholakova, Z. Mitrinova, K. Golemanov, N. D. Denkov, M. Vethamuthu and K. P. Ananthapadmanabhan, Control of Oswald Ripening by Using Surfactants with High Surface Modulus, *Langmuir*, **27**, 14807–14819, 2011.

(52) E. Dickenson, R. Ettelaie, B. S. Murray and Z. Du, Kinetics of Disproportionation of Air Bubbles beneath a Planar Air/Water Interface Stabilized by Food Proteins, *J. Colloid Interface Sci.*, **252**, 202–213, 2002.

(53) A. Dutta, A. Chengara, A. D. Nikolov, D. T. Wasan, K. Chen and B. Cambell, Destabilization of Aerated Food Products: Effect of Oswald Ripening and Gas Diffusion, *J. Food Eng.*, **62**, 177–184, 2004.

(54) E. S. Johnnott, Black Spots in Thin Liquid Films, *Philos. Mag.*, **11**, 746–753, 1906.

(55) J. Perrin, La Stratification des Lames Liquides, *Les Annales de Physique*, **10**, 160, 1918.

(56) L. Lobo and D. T. Wasan, Mechanism of Aqueous Foam Stability in the Presence of Emulsified Non-Aqueous Phase Liquids, *Langmuir*, **9**, 1668, 1993.

(57) I. B. Ivan and D. S. Dimitrov, *Thin Liquid Films*, Vol. **29**, Marcel Dekker, New York, p. 379, 1988.

(58) A. D. Nikolov, and D. T. Wasan, Ordered Micelle Structuring in Thin Foam Films Formed from Anionic Surfactant Solution, 1. Experimental, *J. Colloid Interface Sci.*, **133**, 1–12, 1989.

(59) P. A. Kralchevsky, A. D. Nikolov, D. T. Wasan and I. B. Ivanov, Formation and Expansion of Dark Spots in Stratifying Foam Films, *Langmuir*, **6**, 1180, 1990.

(60) A. D. Nikolov and D. T. Wasan, Dispersion Stability Due to Structural Contribution of the Particle Interactions as Probed by Film Thickness, *Langmuir*, **8**, 2985–2994,1992.

(61) D. T. Wasan and A. D. Nikolov, Foams and Emulsions: The Importance of Structural Forces, *Aust. J. Chem.*, **60**, 633–637, 2007.

(62) V. Bergeron and C. J. Radke, Equilibrium Measurements of Oscillating Disjoining Pressure in Aqueous Foam Films, *Langmuir*, **8**, 3020–3026, 1992.

(63) V. Bergeron, *Forces and Structures in Surfactant-Laden Thin Liquid Films*. PhD, Chem. Eng., University of California, Berkeley. 1993.

(64) V. Bergeron, A. l. Jimenez-Laguna and C. J. Radke, Hole Formation and Sheeting in the Drainage of Thin Liquid Films, *Langmuir*, **8**, 3027–3032, 1992.

(65) D. Henderson, A. Trokhymchuk, A. D. Nikolov and D. Wassan, Computer Modelling of Ionic Micelle Structuring in Liquid Films, *J. Phys. Chem. B*, **107**, 3927–3937, 2003.

(66) A. Trokhymchuk, D. Henderson, A. D. Nikolov and D. T. Wassan, A Simple Calculation of Structural and Depletion Forces for Fluids/Suspensions Confined in a Film, *Langmuir*, **17** (16), 4940–4947, 2001.

(67) D. Henderson, A. Trokhymchuk, A. D. Nikolov and D. T. Wasan, Structure and Layering of Fluids in Thin Films. In *Emulsions, Structure, Stability and Interactions*, Ed. D. Petsey, Elsevier, Chapter 7, pp. 259–311, 2004.

(68) D. T. Wasan A. D. Nikolov D. Henderson and A. Trokhuymchuk, Confinement Induced Structural Forces in Colloidal Systems. In *Encyclopedia of Surface and Colloid Science*, Ed. A. Hubbard, Marcel Dekker, New York, pp. 1181–1192, 2002.

(69) A. D. Nikolov and D. T. Wasan, Nonionic Micellar Films: Thinning and Stability Colloids and Interface Science Series. In *Colloid Stability and Applications in Pharmacy*, Vol. **3**, Ed. T. F. Tadros, Wiley – VCH Verlag GmbH and Co, KGaA, Weinham, 2007.

(70) D. Wasan and A. Nikolov, Thin Liquid Films containing Micelles or Nanoparticles, *Curr. Opin. Interface Sci.*, **13**, 128–133, 2008.

(71) G. Sethumadhavan, S. Bindal, A. Nikolv and D. Wasan, Stability of Thin Films containing Polydispersed Particles, *Colloids Surf., A*, **204**, 51–52, 2002.

(72) K. D. Danov, E. S. Basheva, P. A. Kralchevsky, K. P. Ananthapadmanabhan and A. Lips, The Metastable States of Foam Films Containing Electrically Charged Micelles or Particles; Experiment and Quantitative Interpretation, *Adv. Colloid Interface Sci.*, **168**, 50–70, 2011.

(73) S. K. Bindal A. D. Nikolov, D. T. Wasan, D. P. Lambert and D. C. Koopman, Foaming in Simulated Radioactive Waste, *Environ. Sci.*, **35**, 3941–3947, 2001.

(74) P. R. Garett and P. L. Gratton, Dynamic Surface Tensions, Foams and the Transition from Micellar Solution to Lamellar Phase Dispersion, *Colloids Surf., A*, **103**, 127–145, 1995.

(75) B. Novales and Coworkers, Self-Assembly and Foaming Properties of Fatty Acid-Lysine Aqueous Dispersions, *Langmuir*, **26** (8), 5329–5334, 2010.

(76) L. K. Shrestha and Coworkers, Aqueous Foams Stabilized by Dispersed Surfactant Solid and Lamellar Liquid Crystalline Phase, *J. Colloid Interface Sci.*, **301**, 274–281, 2006.

(77) Z.-L. Chen, Y.-L. Yan and X.-B. Huang, Stabilization of Foams Solely with Polyoxyethylene: Type Nonionic Surfactants, *Colloids Surf., A*, **331**, 239–244, 2008.

(78) K. Koczo, A. D. Nikolov, and D. T. Wasan, Mechanism of Aqueous Foam Stability and Antifoaming Action with and without Oils: A Thin Film Approach. In *Foams, Fundamentals and Applications in the Petroleum Industry, Advances in Chemistry Series*, no. 242, Ed. L. L. Schramm, American Chemical Society, Washington, DC, pp. 47–114, 1994.